Available at www.sciencedirect.com

INFORMATION PROCESSING IN AGRICULTURE xxx (xxxx) xxx

journal homepage: www.keaipublishing.com/en/journals/information-processing-in-agriculture/

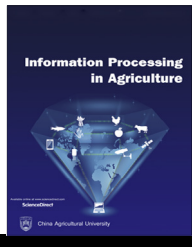

A survey of image-based computational learning techniques for frost detection in plants

Sayma Shammi [a,b], *Ferdous Sohel* [a,b,*], *Dean Diepeveen* [b,c], *Sebastian Zander* [a], *Michael G.K. Jones* [b]

[a] *Discipline of Information Technology, Murdoch University, Murdoch, WA 6150, Australia*
[b] *Centre for Crop and Food Innovation, Food Futures Institute, Murdoch University, Murdoch, WA 6150, Australia*
[c] *Department of Primary Industries and Regional Development, Western Australia, South Perth, WA 6151, Australia*

ARTICLE INFO

Article history:
Received 9 July 2021
Received in revised form
10 February 2022
Accepted 13 February 2022
Available online xxxx

Keywords:
Frost
Cold stress
Machine learning
Image analysis
Crop
Plant

ABSTRACT

Frost damage is one of the major concerns for crop growers as it can impact the growth of the plants and hence, yields. Early detection of frost can help farmers mitigating its impact. In the past, frost detection was a manual or visual process. Image-based techniques are increasingly being used to understand frost development in plants and automatic assessment of damage resulting from frost. This research presents a comprehensive survey of the state-of the-art methods applied to detect and analyse frost stress in plants. We identify three broad computational learning approaches i.e., statistical, traditional machine learning and deep learning, applied to images to detect and analyse frost in plants. We propose a novel taxonomy to classify the existing studies based on several attributes. This taxonomy has been developed to classify the major characteristics of a significant body of published research. In this survey, we profile 80 relevant papers based on the proposed taxonomy. We thoroughly analyse and discuss the techniques used in the various approaches, i.e., data acquisition, data preparation, feature extraction, computational learning, and evaluation. We summarise the current challenges and discuss the opportunities for future research and development in this area including in-field advanced artificial intelligence systems for real-time frost monitoring.

Contents

* Corresponding author at: Discipline of Information Technology, Murdoch University, 90 South Street, Murdoch, WA 6150, Australia.
E-mail address: F.Sohel@murdoch.edu.au (F. Sohel).

Peer review under responsibility of China Agricultural University.
https://doi.org/10.1016/j.inpa.2022.02.003

Please cite this article as: S. Shammi, F. Sohel, D. Diepeveen et al., A survey of image-based computational learning techniques for frost detection in plants, Information Processing in Agriculture, https://doi.org/10.1016/j.inpa.2022.02.003

1. Introduction

Agriculture provides the primary source of food for humans and plays a vital role in economies worldwide. It is anticipated that grain production will need to be doubled by 2050 to meet the increased global demand from population growth [1]. To meet this increased demand, agricultural practices need to adopt smart technologies to ensure better yields [2]. Precision agriculture is a process that uses information and technology with high-resolution spatiotemporal data from atmospheric and soil conditions [3]. Precision agriculture provides farmers with opportunities by enabling remote monitoring technologies and targeted management for high yields and risk mitigation.

However, significant reductions in crop yield can occur due to adverse environmental events. Frost is a significant weather event that directly impacts plant growth and flowering, hence yields. In recent years, frost events have increased

Please cite this article as: S. Shammi, F. Sohel, D. Diepeveen et al., A survey of image-based computational learning techniques for frost detection in plants, Information Processing in Agriculture, https://doi.org/10.1016/j.inpa.2022.02.003

in frequency [4,5]. These events cause substantial economic damage by limiting the growth of both wild and crop plant species. In Europe and North America, late-frost damage causes more economic losses to agriculture than any other hazard related to climate [6,7]. In 2017, a single late spring frost caused economic losses in Europe of 3.3 billion Euros [8]. Frost damage costs the grains industries of Australia an estimated $360 million annually [9]. Hence, early frost detection technologies with appropriate decision support systems can help to mitigate the impacts of such adverse frost events.

For detecting the effects of frost-damage, quantifying techniques such as, frost exclusion chambers with active heating can be used to compare damaged and non-damaged crops [10]. However, temperatures are commonly measured near the crop canopy and field-scale to determine the crops' exposure to frost [11,12]. Imaging-based techniques offer a non-destructive method for detecting frost-damage in plants. Imaging provides extra insight for understanding freezing and shows ice formation on the plant surface to clarify the nature of the damage. Various imaging types, such as thermal and spectral, can be used to screen for frost in plants. This functionality is essential for early detection to enable frost risk management, especially at field-scale. This could limit economic losses by making timely operational decisions, including changing harvest strategies [13] or when to cut the crop for forage [10].

At present, researchers manually investigate the ice nucleation and freezing patterns inside plants [14,15]. However, recent implementations of imaging-based systems with computational approaches are being used more widely. Computational approaches allow mathematical models to study the behaviour of a complex system by computer simulation. For example, statistical analysis is one of the computational approaches that is being used in frost analysis [16,17]. The use of traditional machine learning (ML) and deep learning (DL) techniques for frost detection is increasing. Statistical methods can be used to analyse variations of the patterns in the image data. Traditional ML techniques can estimate the outputs based on feature extraction and training the models. DL techniques use many layers of artificial neurons that transform the input images into outputs by learning deep features. Because of their promising performance, imaging-based ML and DL techniques are being used more widely in automatically counting of grain ears or spikes, for yield estimation, and for analysing the impact of frost damage [18–20].

The research presented here provides a comprehensive survey of the papers on imaging-based frost detection in plants and crops over the last ten years. We propose a taxonomy and classify 80 papers related to frost detection and analysis in plants. We have summarised these papers (in Table 3) with the acronyms from the taxonomy, and categorised them according to the computational method applied. We have also categorised them according to their image modality, image collection, pre-processing, and feature extraction techniques. In this review, we discuss the techniques including image acquisition, preparation, feature extraction, and classification methods. We also provide an overview of different evaluation metrics were used to determine the efficiency of image-based detection techniques. Overall, our taxonomy aids the categorisation and a summation of a large number of publications on image-based frost detection.

The remainder of the paper is organised as follows: Section 2 justifies the importance of this survey. It first discusses the review articles on frost detection and analysis. It then highlights that there is no survey paper on image-based frost detection using computational learning methods. Although the focus of this survey is on image-based computational models, for the sake of completeness, in Section 3 we briefly cover the prior art (e.g., pre 2010). It indicates the works were mainly done via manual inspection. Section 4 describes the criteria used for selecting the papers that are thoroughly reviewed in this survey. In Section 5, the image modalities are discussed in detail as a component of the frost detection techniques. Section 6 discusses the overall process of computational frost detection. In Section 7, we present the taxonomy and in Section 8 the popular computational methods used in image-based frost detection are described. Subsequently, we summarise the 80 articles based on frost detection and analysis in plants in Table 3. Various evaluation metrics for statistical, ML and DL methods are discussed in Section 9. In Section 10, we discuss the data sets used in the papers covered in this survey. In Section 11, we discuss current and future opportunities and the challenges in image-based automated frost detection in crops. The paper is concluded in Section 12.

2. Related surveys

The study of freezing mechanisms in plants has long been an interest to researchers. Fennell [21] summarised the mechanisms of freezing tolerance in grapevines concerning the influence of genotype, phenological development, and environmental factors. Neuner [22] reviewed the key components of frost resistance in alpine woody plants. Their report reviewed complex and diverse ways to survive the frost damage. On the other hand, Ambroise et al. [23] reviewed the root causes of freezing stress in plants, and discussed the root level of plant frost damage-inducing cold hardiness. In addition, their paper included the plants' metabolic and molecular responses depending on plant age, category and species. They also discussed how the roots sense frost and environmental signalling for cold acclimation. Their discussion was limited to molecular analysis of plant frost effects, but advanced computational techniques were not used to address them.

Imaging techniques have been more commonly used for frost detection in plants. Humplík et al. [24] reviewed RGB, chlorophyll fluorescence, thermal and hyperspectral imaging for phenotyping plant stress response. Their study only covered a few articles related to cold stress, rather they focused on drought stress. Recently, Yu and Lee [25] reviewed methods available for evaluating the freezing injury in temperate fruit trees. They discussed the visual evaluation, thermal analysis, electrolyte leakage analysis, and Triphenyl tetrazolium chloride (TTC) reduction analysis for evaluating freeze injury. Their review was limited to temperate fruit trees and also to textual data, and did not discuss any other image-based computational approaches. Gao et al. [26] showed that DL-based

Please cite this article as: S. Shammi, F. Sohel, D. Diepeveen et al., A survey of image-based computational learning techniques for frost detection in plants, Information Processing in Agriculture, https://doi.org/10.1016/j.inpa.2022.02.003

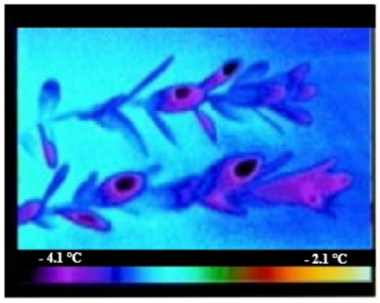

(a) Initiation of ice nucleation.

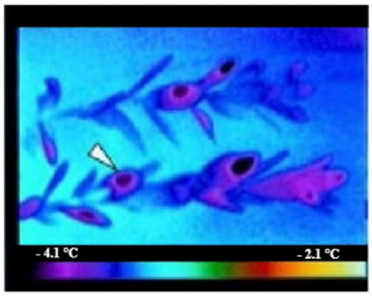

(b) Ice propagation started from bacterial droplet (indicated by arrow) to leaf and stem.

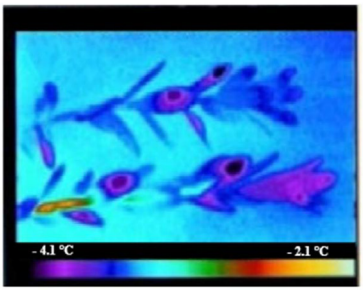

(c) Ice propagation along the stem entering other leaves

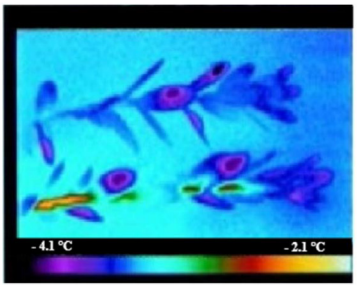

(d) Ice propagation from nucleation site to terminal leaf via the stem.

Fig. 1 – One of the earliest ways of observing freezing in cranberry plants using infrared thermography [15]

Table 1 – Total number of retrieved articles for the keywords indicated.

No.	Digital library	Search query	Number of retrieved documents
1.	Google Scholar	[[[“Frost” OR “Freeze” OR “Cold Stress”] AND “Damage”]] AND [“Crop”AND “Imaging”] AND [“Statistical Analysis” OR “Machine Learning” OR “Deep Learning”]	972
2.	Scopus	TITLE-ABS-KEY (“Frost” OR “Freeze” OR “Cold Stress”) AND (“Crops”OR “Plants”) AND (“Image” OR “Imaging”) AND (“Statistical Analysis” OR “Machine Learning” OR “Deep Learning”)	110
3.	ScienceDirect	(“Frost” OR “Freeze” OR “Damage”) AND (“Crops” OR “Plants”) AND(“Image” OR “Imaging”) AND (“Statistical” OR “Machine Learning”)	60
4.	SpringerLink	‘(“Frost Damage”) AND (“Crops”) AND (“Imaging”) AND (“StatisticalAnalysis” OR “Machine Learning” OR “Deep Learning”)’	23
5.	MDPI	(“Frost Damage”) AND (“Crops”) AND (“Imaging”) AND (“StatisticalAnalysis” OR “Machine Learning” OR “Deep Learning”)	27
6.	Murdoch University Library	(TitleCombined:(\(“Frost” OR “Freeze” OR “Cold Stress” OR \)) AND (\(“Image” OR “Imaging” \) AND (Abstract:(\(“Crops” OR “Plants” \))AND (\(“Statistical Analysis” OR “Machine Learning” OR “Deep Learning” \))	38

Please cite this article as: S. Shammi, F. Sohel, D. Diepeveen et al., A survey of image-based computational learning techniques for frost detection in plants, Information Processing in Agriculture, https://doi.org/10.1016/j.inpa.2022.02.003

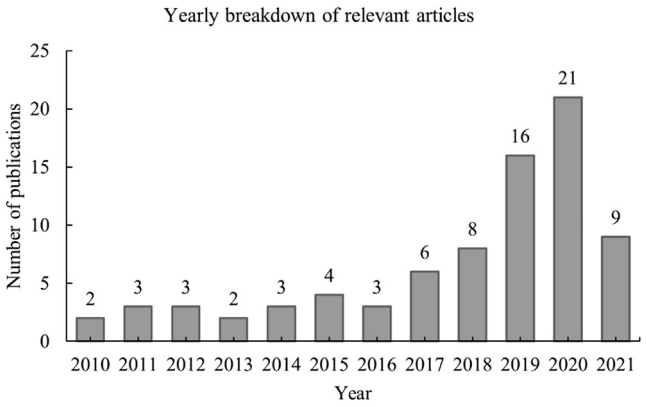

Fig. 2 – The number of selected papers on image-based plant frost detection from 2010 (January) to 2021 (March).

plant stress diagnosis could be deployed in crop stress imaging and phenotyping tasks. Their study explained that imaging systems could be required for non-destructive approaches in precision agriculture. They discussed imaging and deep learning principles. However, their study focused on other abiotic stresses rather than on cold stress.

Fitzgerald et al. [10] reviewed both active and passive methods for early frost damage quantification. Their study discussed remote sensing for cold stress mapping techniques. They also described non-destructive approaches such as spectral reflectance and spatial distribution of temperature to identify frost in crops. They focused on different field-based methods used for early frost detection. Barlow et al. [27] reviewed current knowledge on the impacts of frost on wheat production and how these impacts are incorporated into contemporary process-based crop models.

Most of the existing reviews focused either on imaging or ML techniques [28] for biotic stress detection, but not on frost damage. For instance, Pineda et al. [29] published a review article for detecting biotic and abiotic stress from thermal images. The study reported that thermography is more efficient than traditional image processing methods for detecting plant stress. They also mentioned that thermography

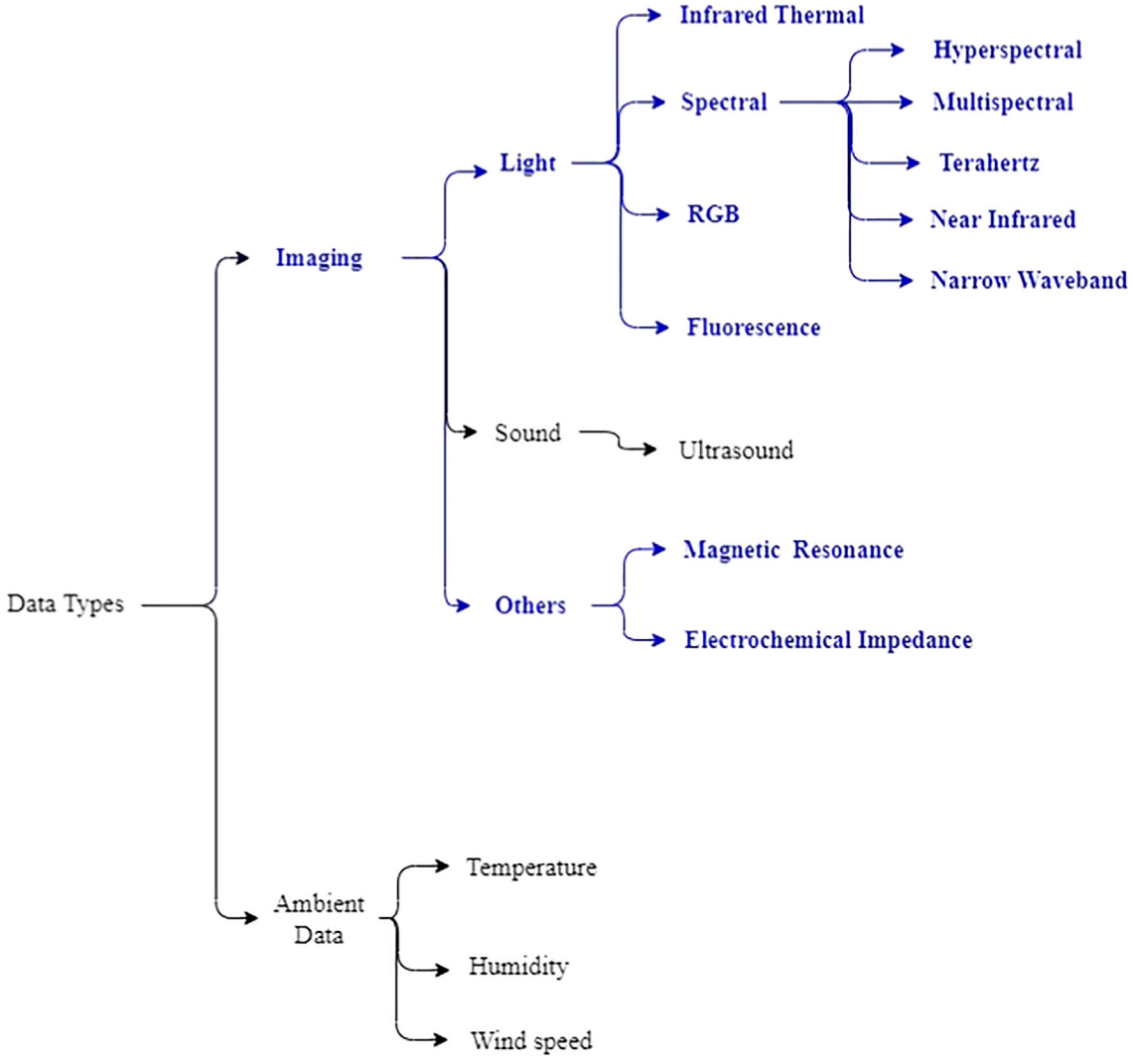

Fig. 3 – An overview of various data modalities for plant frost detection (best viewed in colour). The coloured branches are discussed in this review.

Please cite this article as: S. Shammi, F. Sohel, D. Diepeveen et al., A survey of image-based computational learning techniques for frost detection in plants, Information Processing in Agriculture, https://doi.org/10.1016/j.inpa.2022.02.003

requires corrections to achieve an accurate interpretation of the stress. In their review, they covered thermography for plant stress detection. Most importantly, this study did not adequately cover the breadth and depth of the literature for detecting frost stress specifically. Some studies reviewed other techniques for evaluating frost injury at the molecular level without using any ML or statistical approaches. It is evident that, with the rapid development of digital sensing technologies, low cost capturing of high-quality imaging data has become more accessible. Therefore, in the past decade, there have been many research articles based on computing hardware as well as image processing, computer vision techniques, and decision support for stress detection. There is also a continuous growth in research articles, both in terms of quality and use of diverse and contemporary tools and methods to detect plant stress. However, there is still a research gap in implementing these technologies in detecting frost in plants. To the best of our knowledge, there is no review article in which plant frost damage has been detected or quantified with the help of imaging and computational methods. Given the breadth, depth and contemporary development of the field, a comprehensive review of the contemporary literature is justified.

3. Early days of image-based frost detection in plants

In studies before 2010, freezing patterns in crops and wild plants were observed visually thermal images [14,30,31]. For example, Ceccardi et al. [32] studied the freezing mechanisms through differential thermal analysis in 1995. Their method incorporated infrared thermography to visualise exothermic

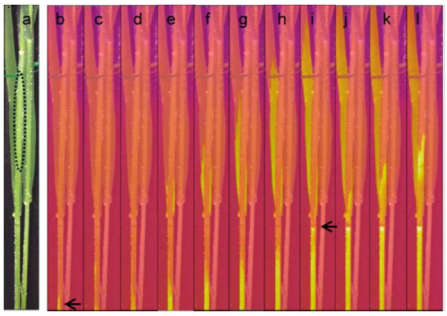

(a) Infrared thermal ([35]).

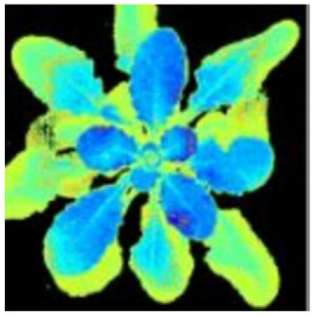

(b) Chlorophyll fluorescence ([16]).

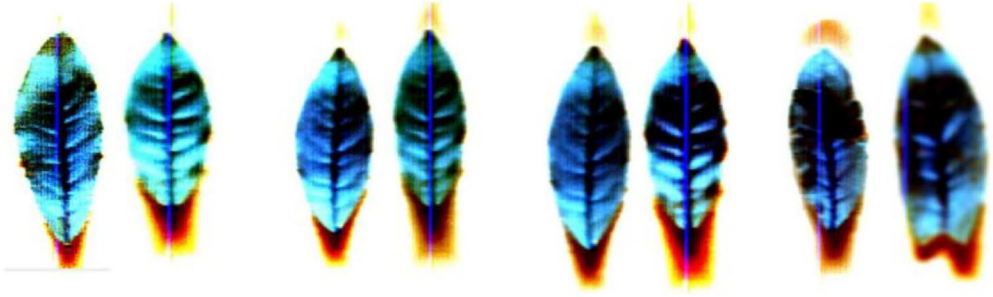

(c) Hyperspectral reflectance ([17]).

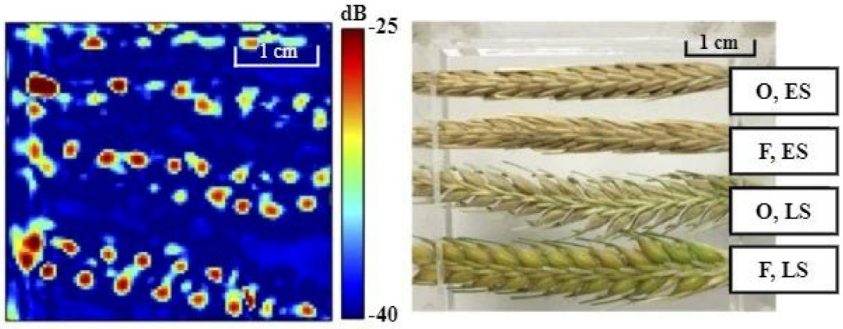

(d) Terahertz (left) and optical RGB image (right) ([57]).

Fig. 4 – Examples of various image modalities.

Please cite this article as: S. Shammi, F. Sohel, D. Diepeveen et al., A survey of image-based computational learning techniques for frost detection in plants, Information Processing in Agriculture, https://doi.org/10.1016/j.inpa.2022.02.003

events in jojoba. Wisniewski et al. [14] demonstrated infrared thermography as an excellent method for studying ice nucleation and plant propagation. In their research, monitoring of an array of plant species under different freezing conditions revealed that ice nucleation and propagation are readily observable by thermal video.

Workmaster et al. [15] provide evidence that stomata are the probable avenue through which ice penetrates into cranberry leaves. However, the cuticle on the adaxial leaf surface provides an adequate barrier to ice propagation. This valuable observation was also supported by infrared video thermography. In Fig. 1, their observation of ice nucleation and propagation is explained in sequential images. Ice nucleation started from the bacterial droplet and propagated through the stem to the terminal leaf. Pearce and Fuller [31] investigated the freezing of barley by using infrared video thermography. In laboratory tests with barley, initially, an interesting observation was made. Ice spreading delayed from the crown to the leaves and roots, while ice propagated through the leaf to the rest of the plants. Wisniewski et al. [33] used infrared thermography to study the freezing behaviour of extrinsic nucleating agents. These are agents which can cause freezing at warmer temperatures. In 2003, the utility of infrared imaging was examined for detecting freezing events in whole turfgrass plants [30].

Although computational methods were not widely available only a few years ago, researchers were nevertheless able to demonstrate that thermal videography was a potential tool for visualising the freezing patterns in real-time [15,30,33]. This valuable observation led to an understanding that the formation and propagation of ice inside plant tissues, and opened the door for more research in this area.

4. Paper selection criteria for this survey

Our central research theme was: What is the role of imaging associated with the state-of-the-art techniques for detecting and analysing frost in crops? For selecting the papers, we followed three main steps: (i) a search for related papers, (ii) selection of the most relevant papers and (iii) detailed analysis of these papers. In this research, we provide a comprehensive survey of image-based computational learning techniques for frost detection in plants. In Section 3, we briefly summarised the traditional techniques used for image-based frost detection. The focus of this paper is however, on image-based computational models for frost detection and analysis. We have included papers published since 2010, when computational models started to be popularly used in frost detection. We used a keyword-based search strategy across all major digital libraries and indexing repositories to collect related work based on this research question. We searched Google Scholar, Scopus, ScienceDirect, SpringerLink, Multidisciplinary Digital Publishing Institute (MDPI), and Murdoch University Library databases for journal articles and conference papers. We limited the search to between January 2010 and March 2021. Table 1 shows the number of papers found from the search queries.

We then combined all the identified papers and removed duplication, which resulted in a total of 1 054 papers. However, the search returned a large number of papers covering post-harvest freeze damage, disease and other stress detection, crop growth and quality monitoring through imaging, and food storage. These papers are not the primary focus of this study (although they are relevant in other contexts). Therefore, we considered that these papers were not relevant for our review, as the focus is on investigating frost-damage in agricultural crops. In addition, we sought papers that used images as a data type, and which applied at least one computational method. As a result, we manually selected the papers that focused on detecting and analysing frost issues in plants from images as the final step.

The bar graph in Fig. 2 shows the yearly count of relevant articles for the search query from 2010 to 2021 (March). In this study, we only reviewed these articles. It can be seen in Fig. 2 that, before 2018, the number of publications related to image-based computational methods for frost damage analysis was quite low. Moreover, Fig. 2 shows there has been an upward trend in recent years, i.e., since 2018. Therefore, we reviewed the publications from 2010 to March 2021 to understand how image-based frost detection and analysis techniques (in crops and wild plants) have evolved during this period.

5. Overview of image modalities

A critical component of determining frost in plants is the type of data that is used. In this context, data can be image and ambient, such as temperature, humidity and wind speed. According to the literature review, researchers have used various image modalities as data types for visual and automatic evaluation. Therefore, the scope of this study is limited to image-based computational methods. In Fig. 3, we propose a tree to show various data modalities, where a summary of the different image types is also illustrated. We can divide the image modalities into three categories: light, sound and others. Light-based techniques can be further split into subgroups. We only cover the highlighted branches of the tree as shown in Fig. 3. In the following subsections, we discuss the commonly used image modalities for frost detection.

5.1. *Infrared thermal*

Infrared thermography offers a view of temperature differences or thermal properties of subsurface measurements. Modern thermal cameras can convert the information gathered from the infrared spectrum into true colour graphical images with temperature levels represented by different colour palettes [34]. Infrared thermography can be used to study the freezing mechanism inside plant tissue [35–38] and ice nucleation [39–41].

In addition, thermography can be used to capture the propagation of ice formation inside plant leaves, and stem [35,40]. Neuner [22] and Hacker et al. [37] measured temperatures and freezing patterns throughout the freezing experiments with FLIR S60. In Fig. 4(a), the freezing progression of a wheat plant is shown [35]. In this figure, the wheat plant went through ice nucleation and propagation from b to l (the notations are shown at the top part of the figure). Hoer-

Please cite this article as: S. Shammi, F. Sohel, D. Diepeveen et al., A survey of image-based computational learning techniques for frost detection in plants, Information Processing in Agriculture, https://doi.org/10.1016/j.inpa.2022.02.003

miller et al. [42] monitored cooled Arabidopsis thaliana plants with a FLIR thermal camera. Livingston et al. [40] used a High-Definition FLIR SC8303 sensor to collect images of 1 280 × 720 pixels of wheat plants freezing. Kokin et al. [43] recorded thermal radiation to measure the temperature at >40 000 points on the leaf surface. A high-resolution thermal camera (DJI Zenmuse XT2 with a 19 mm lens) by Yuan and Choi [44] was deployed to achieve radiometric functionalities and to map the temperature in an apple orchard for timely frost management.

5.2. *Spectral*

Spectral imaging uses multiple bands across the electromagnetic spectrum. For example, frost damage can be assessed through spectral imaging sensors [19]. According to Fitzgerald et al. [19], physiological changes can occur in plants, including damage to photosynthetic processes and physical damage to tissues, which can potentially manifest as changes in plant colour detected using spectral sensors. In the following subsections, we discussed various subgroups of spectral imaging.

5.2.1. *Multispectral*

Multispectral imaging captures data within specific wavelength ranges across the electromagnetic spectrum. Multispectral images were used to determine the impact of frost by many researchers [20,45–47]. Goswami et al. [47] and Jelowicki et al. [46] chose medium resolution multispectral images covering 13 spectral bands, from 0.443 to 2.190 μm. To distinguish frost affected areas of plants using multispectral cameras, four different spectral bands: green (530–570 nm), red (640–680 nm), red edge (730–740 nm), formed the multispectral data. Jelowicki et al. [46] also investigated the influence of spatial resolution of the multispectral data to estimate the damaged area. Goswami et al. [47] recorded the multispectral images in the central wavelength in green, red, red edge and NIR channels for further pre-processing.

5.2.2. *Hyperspectral*

Although hyperspectral imagery is a part of the multispectral spectrum, it consists of a large number of narrow bands (10–20 nm) in the electromagnetic spectrum. From such images, useful spectral information is extracted for plant phenotyping. Lacoste et al. [48] used hyperspectral images consisting of 64 000 pixels, acquired from 240 spectral bands from 392 to 889 nm (spectral resolution 2.1 nm) by 640 pixels (spatial) from the flag leaves of 15 wheat plants. Wei et al. [49] collected leaf spectra from the wavelength range between 400 nm and 2 400 nm. Canopy reflectance measurements were made using ASD Field Spec FR, ASD Inc., resulting in libraries of spectra from 350 to 2 500 nm [13,19,50]. Feng et al. [50] measured this data before freeze injury and 5, 10, 20, 35 days after freeze treatment.

Fitzgerald et al. [19] collected data for the *meta*-analysis at the canopy, head, and leaf scales to represent canopy variability. Asante et al. [17] utilised hyperspectral data to see the cold tolerance difference to nitrogen treatment. Hyperspectral reflectance images of frozen tea leaves with different nitrogen concentrations are shown in Fig. 4(c). According to Lu et al. [51], Spectralon fluoropolymer was used to standardise the spectral responses of the hyperspectral images. The hyperspectral images were acquired over the wavelength range of 390–1000 nm (at 462 wavelengths). Zhang et al. [52] studied frost damage characteristics from the hyperspectral images with a spectral range of 400–1000 nm. Hyperspectral sampling of plant components was conducted with a PIKA II hyperspectral camera [20,53]. Shao et al. [54] composed the hyperspectral image at a spectral resolution of 5 nm. The imaging sensor used by Gao et al. [55] had spectral ranges of 517–1 729 nm. Choudhury et al. [56] measured high-resolution spectral reflectance of vegetation and soil in field and laboratory conditions covering the 350 –2500 nm spectral region.

5.2.3. *Near infrared spectral*

Near-infrared spectral (NIRS) imaging is captured from the near-infrared region of the electromagnetic spectrum (from 780 nm to 2 500 nm). Near-infrared spectral data was used to distinguish frost-damaged seeds and kernels [58,59]. Agelet et al. [58] measured 141 spectral points ranging from 850 nm to 1 650 nm, at 5 nm intervals. However, Jia et al. [59] used a total of 633 wavelength points from 1 110–2 500 nm, where they showed that NIRS is feasible to analyse frost-damaged kernels. Agelet et al. [58] also discussed the limitations of NIRS. They argued that NIRS is only suitable for single-seed analysis because of the variation between single-seeds within a plant head. The performance also degrades for high concentrations due to its detection limitations.

5.2.4. *Narrow waveband spectral*

Narrow waveband spectral images provide detailed and accurate information by capturing precise measurements of specific wavelengths. Wu et al. [60] adopted a new spectral image for predicting frost-damaged yield loss during stem elongation in wheat. The images were captured between 1 400 and 2 100 nm wavebands. They demonstrated that a narrow band could determine the optimal spectral index for predicting yield loss caused by frost.

5.2.5. *Terahertz*

Frost damage assessment through terahertz imaging is a relatively new technique. Terahertz imaging is non-ionizing and can penetrate most dry and non-metallic materials. According to Lee et al. [57], the terahertz images were collected at 275 GHz and 10 000-pixel resolution. This technique provided additional information in the images of the spikes for grain water content. Their imaging technology is shown on the left side of Fig. 4(d).

5.3. *Rgb*

An RGB image is a colour image captured in the range of the visible electromagnetic spectrum. The image is reproduced from red, green, and blue light reflected from the object. RGB is the most popular and well-known imaging technique. An RGB image captures the visible symptoms of frost damage. Such images have been used to identify the frost-damaged areas of plants after a few days after a frost [61,62]. Macedo-Cruz et al. [61] captured RGB images of healthy and frost-damaged areas of oat crops. The colour differs from the green-healthy crop to the frost-damaged discoloured crops.

Please cite this article as: S. Shammi, F. Sohel, D. Diepeveen et al., A survey of image-based computational learning techniques for frost detection in plants, Information Processing in Agriculture, https://doi.org/10.1016/j.inpa.2022.02.003

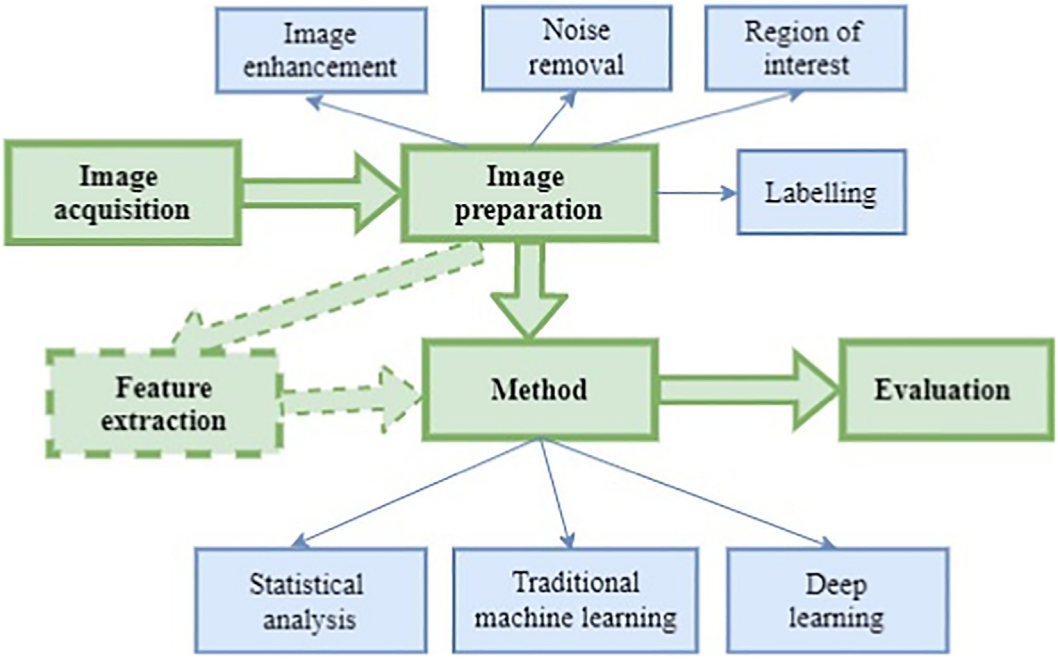

Fig. 5 – Summary of the workflow of image-based frost detection techniques. The green rectangles indicate the key steps, and the blue ones show the possible branches to perform the respective steps. (For interpretation of the references to colour in this figure legend, the reader is referred to the web version of this article.)

HamidiSepehr et al. [62] applied a similar strategy. However, L´opez-Granados et al. [63] captured sequential RGB images to monitor flowering dynamics of almond trees to reduce frost risk. Furthermore, RGB images can also be an efficient technique for frost management [44]. They used high-resolution (1920 × 1080) RGB images and thermal images to determine the heating requirements in an apple orchard. Kimball et al. [64] used RGB images to compare and evaluate the green cover and accuracy of their visual ratings of frost severity.

5.4. *Fluorescence*

Fluorescence imaging helps visualise biological processes taking place in plants. For example, fluorescence images are used to characterise frost damage in crops and plants [65]. Perry et al. (2017b) explored four excitation bands (ultra-violet, blue, green, and red) and three detection bands (yellow, red and far-red). They combined both activation and detection wavelengths for the measurements of frost indices. Fluorescence microscopy was adopted by Livingston et al. [66] to understand the survival mechanism of freezing in oat crowns. This technique revealed that the frozen tissues emitted fluorescence with excitation between 405 and 445 nm wavelengths.

5.4.1. *Chlorophyll fluorescence*

Chlorophyll fluorescence is one of the widely used modalities to assess chilling injury [16,67,68]. Chlorophyll fluorescence imaging can capture plant stress parameters and spatial heterogeneity distribution [69]. Dong et al. [70] used chlorophyll fluorescence images and fluorescence parameters to find chilling injury in tomato seedlings. In an extended research article by Dong et al. [67], they used chlorophyll fluorescence to discriminate different types of cold stress.

Combinatorial chlorophyll fluorescence imaging can differentiate cold tolerant and sensitive accessions [16]. A chlorophyll fluorescence image from their work is in Fig. 4 (b). Fluorescence emission can provide highly contrasting features to reveal plant tolerance to low temperatures [71]. On the other hand, Arnold et al. [68] suggested considering chlorophyll fluorescence when there is a clear understanding of plants' tolerance to temperature extremes.

5.5. *Others*

A few other image modalities have been used to analyse frost in plants. Electrical impedance tomography (EIT) and reflected light microscopy are the two other image modalities used in frost detection, as illustrated in Fig. 3. Electrical impedance tomography (EIT) has rarely been used to study plant freezing. Qian et al. [72] explored EIT to identify the freezing resistance in rose stems. They used different excitation currents such as 100, 150, 200, 250, 300 and 500 micro amperes (μA), but the best image was constructed when the size and frequency of the excitation current were 250 μA and 1 kHz. Stegner et al. [73] detected ice inside plant tissues from reflected light microscopy. They observed glowing light reflections from the ice crystal. Magnetic resonance imaging has also been used [74].

6. Image-based computational approaches for frost detection and analysis

Image-based computational approaches have a typical workflow of image acquisition, preparation, feature extraction, computational model application, and model evaluation

Please cite this article as: S. Shammi, F. Sohel, D. Diepeveen et al., A survey of image-based computational learning techniques for frost detection in plants, Information Processing in Agriculture, https://doi.org/10.1016/j.inpa.2022.02.003

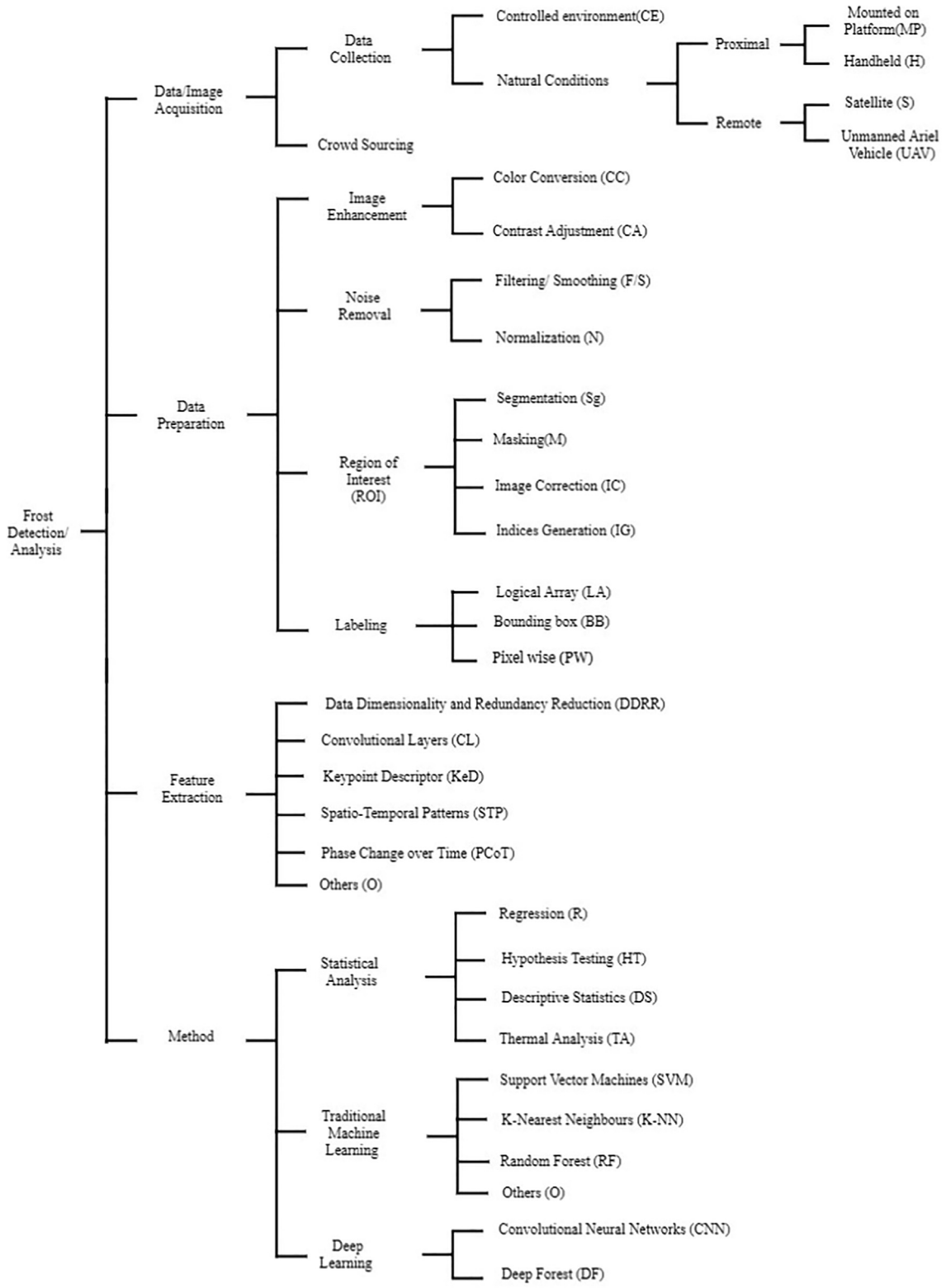

Fig. 6 – The taxonomy of image-based frost detection techniques. We have used acronyms for the leaf components, which were also used in Table 3.

[17,53,75–77]. In Fig. 5, a summary of the workflow is provided for frost detection and analysis techniques. The green rectangles represent the key steps and green arrows show the respective workflow. The blue rectangles represent possible ways to accomplish the respective steps. The dashed lines with respect to the "Feature extraction" step indicate that some methods may not use this step, and rather operate directly on the image data.

Please cite this article as: S. Shammi, F. Sohel, D. Diepeveen et al., A survey of image-based computational learning techniques for frost detection in plants, Information Processing in Agriculture, https://doi.org/10.1016/j.inpa.2022.02.003

The first step is data acquisition. In a specific image-based implementation, image acquisition can be remote or proximal [19,40,52,78]. Different image acquisition devices provide image qualities to capture the desired images, such as thermal, RGB, and hyperspectral cameras [35,61,79]. The image quality is also dependent on how the cameras are mounted on the platforms.

The images usually require pre-processing before they can be used by any computational method. Different image processing techniques have been applied for frost damage detection [51,67,80,81]. Prediction models are built depending on the most relevant features [51,58,59,82,83]. For RGB images, a common feature type is colour [61–64]. Other feature types include spectra, texture and temperature [43,49,65,67,84]. Infrared thermography is used to capture the exothermic features [35,36].

Traditional computational approaches such as statistical and ML-based techniques depend on the selected features from the acquired images. A feature extraction method is required based on the type of feature and the data type. The success of statistical and ML models depends on their ability to identify a hierarchy of features and generalised trends from the available data. Feature extraction tools have also been demonstrated for integrating disparate and redundant data to draw coherent patterns for identification, and quantification [49,85]. The performance of the statistical and ML models rely on the quality of the features. Feature extraction removes redundant information to obtain the most valuable information or clues [83]. As the dimensionality increases, the computational cost also increases. Therefore, it is necessary to find a way to reduce the number or dimension of features being considered [86]. On the other hand, deep learning models can learn suitable features automatically. A convolutional neural network (CNN) is a type of artificial neural network that is usually designed to extract features from the data and classify the high dimensional data [53,87]. The network structure can learn distributed feature representations of data by combining lower level features to form more abstract, higher-level characteristics or features for classification [88]. These abstract and invariant features of the data can be extracted as an essential deep feature [89].

Many statistical, traditional machine and deep learning methods have been used to detect frost damage. The most frequently used statistical models are regression, correlation, significance test [50,67,78,90]. Research related to infrared thermography for frost detection and analysis often apply infrared differential thermal analysis (IDTA) to see the changes in plants over time [12,37–39,42,43]. More recently for frost detection, ML models are used more widely. For example, several researchers classified frost using Support Vector Machines (SVM), a traditional ML model [58–60,91]. The crucial components of an ML model are a moderate-sized data set, an algorithm, feature extraction and a training component [92]. Other ML models such as K-Nearest Neighbors (K-NN), Regression, Artificial Neural Networks (ANN) will be discussed in more detail in Section 8.

Deep learning is currently being actively used for high throughput plant phenotyping. Although CNNs are used for analysing and classifying images, these models require properly labelled images. A typical convolutional network is a stack of convolutional layers. The term convolution means filtering, so each layer refines the input data, convolves them, and feeds the output to the next layer. This process simplifies the data for better processing. Furthermore, a DL network has some key components, such as convolutional layers, pooling layers, activation functions, dense or fully connected layers [93]. A few recent publications have applied DL models for cold stress in plants [53,83].

Evaluation is required to validate the performance of the models. The most commonly implemented evaluation metrics to validate the performance of statistical models are maximum likelihood, correlation or determination co-efficient [20,79]. On the other hand, confusion matrix, precision, recall and F-score are widely used to evaluate ML models [58–60,91]. Intersection over Union (IoU) and mean average precision (mAP) are routinely used evaluation metrics for deep learning models [44,53]. The metrics compare the predictions with ground truth, and generate quantitative scores of performance.

7. Taxonomy of frost detection and analysis techniques

A well-designed taxonomy helps to fit and review different papers in the proposed context. We developed a novel taxonomy based on a typical workflow summary. We divided each key step of the workflow (Fig. 5) based on the surveyed papers. An overall taxonomy of frost detection techniques is shown in Fig. 6. The taxonomy helps to categorise the papers and their underlying techniques into different categories from various viewpoints. We have summarised 80 papers based on the taxonomy shown in Table 3 In this table, we have used the acronyms at the end of each leaf from the taxonomy. We also have categorised the papers based on the crop, image modality, feature extraction and the computational method in Table 3.

This taxonomy has been used to summarise the table in an organised way. For instance, the first paper [60] indexed in Table 3 applied partial least squares regression (PLSR) and Support Vector Regression (SVR) as statistical analysis to predict percent yield difference of damaged wheat based on narrow waveband spectral images. The data set size varied between 77 and 112, and the prediction of frost damage was based on spectral features. The last column in the table uses the acronyms of the taxonomy leaf nodes; as such, this study used a controlled environment (CE) for data collection, smoothing (S) and normalisation (N) for noise removal in the data preparation step. In addition, to extract the region of interest (ROI), reflectance-based indices (IG) for various spectra were generated, and the data were labelled data pixel-wise (PW). Finally, two regression (R) analyses, namely, PLSR and SVR were applied. This classification essentially summarises the basic building blocks of the paper. All the papers indexed in Table 3 are classified in the same way. In the following sections, we discuss the taxonomy branches in detail.

7.1. *Data acquisition*

Frost detection and analysis techniques require sufficient data. Data can be collected either using sensors or crowd-

Please cite this article as: S. Shammi, F. Sohel, D. Diepeveen et al., A survey of image-based computational learning techniques for frost detection in plants, Information Processing in Agriculture, https://doi.org/10.1016/j.inpa.2022.02.003

sourcing. Crowdsourcing can be defined as data collection from outsourcing tasks to many non-professionals [94]. Crowd-sourcing is being increasingly used in scientific research and applications. This type of data collection method is contributing to big data analytics in agricultural research and development projects [95]. In addition, advanced cameras and data loggers can capture data in different modalities. We discuss possible ways of data collection for frost detection and analysis.

7.1.1. *Controlled environment*

For frost analysis, controlled environments (CE) include controlled growth rooms or greenhouses for optimised plant-growing systems and sample preparation. Controlled frost treatments are conducted in an artificially controlled environment [17,60]. Generally, image acquisition inside these controlled environments is defined as proximal sensing. Hyperspectral imaging systems are often used to collect images after the freezing treatment on the mobile electric platform controlled by software and adopt the push-broom method [83,96]. A push-broom method is done by arranging the sensors perpendicular to an object's direction. Gao et al. [55] also used a similar method. Their system uses a push-broom imaging spectrograph at a distance of 38.4 cm from the object. A push-broom hyperspectral camera, PIKA II, was used, which was mounted on a linear gear slider and a Dayton DC gear motor [53].

Alternatively, Dong et al. [70] collected fluorescent images with a chlorophyll imaging system–IMAG-MAX/B inside an artificial climate chamber. A hyperspectral imaging system named Dualix spectral Imaging was used to capture hyperspectral images [97]. Shao et al. [54] acquired the NIR hyperspectral images with SpectralSENS. A DSLR Camera (Nikon D5 100) with an 18–55 mm lens was mounted on a Provista 7 518B Tripod that produced the digital images [80]. To represent canopy variability as input data, Fitzgerald et al. [19] collected spectral images from the head, canopy and leaf with an ASD Field Spec spectrometer. The images were collected by routing the probe into the freezer while undergoing treatment [49]. On the other hand, Duddu et al. [84] used a 10-bit monochrome CCD camera as an imaging spectrograph. Hyperspectral images were collected with artificial lighting, mounted on either side of the lens of the Perten DA 7 200 NIR system in a room with controlled temperature [58]. Arnold et al. [68] obtained their images from a Pulse Amplitude Modulation (PAM) chlorophyll fluorescence imaging system mounted 185 mm above the Peltier plate.

Thermal cameras from the FLIR are often used to collect thermal images [22,35,62]. FLIR cameras come with FLIR Research IR software where the thermal images can be visualised and analysed [62,98]. Neuner [41] took close up thermal images collected by a Therma-CAM S60 camera.

7.1.2. *Natural conditions*

In field environments, frost assessment is required for the early prediction of yield loss. Non-destructive proximal or remote sensing techniques can make rapid, spatial assessment of frost damage [65]. Thus collecting images from field conditions is a crucial step to limit economic losses through timely management decisions [12].

7.1.2.1. *Mounted on platform*.

Cameras are often mounted on platforms to collect images from field-grown crops. For example, Macedo-Cruz et al. [61] placed a digital camera 1.5 m above the ground. Feng et al. [50] placed the probe vertically downward at the height of 0.5 m from the canopy. Similarly, Ma et al. [81] oriented the camera vertically downwards over the canopy at a distance of 1.5 m. on a tripod.

7.1.2.2. *Handheld*.

Canopy reflectance was measured by a handheld spectroradiometer [12,13,79]. Nuttall et al. [12] and Perry et al. [13] used an ASD fieldSpec FR to measure spectral reflectance after the frost treatments. Nuttall et al. [12] also measured fluorescence with a handheld active light fluorometer.

7.1.2.3. *Satellite*.

Recently, high-resolution satellite images have been employed to assess frost risk in cultivated lands, i.e. moderate resolution imaging spectrometer (MODIS) and medium resolution imaging spectrometer (MERIS) images [99]. Currit and St Clair [100] studied MODIS images to evaluate the spatial pattern and the magnitude of damage in the Aspen forests due to spring freeze. Liu et al. [75] and Cogato et al. [45] used Sentinel- 2A/B images for further processing and analysis. Fayad et al. [101] collected sentinel-1 time-series images. Gobbett et al. [102] studied the influence of temperature for frost risk from Landsat 5 TM images. The spatial resolution of Landsat images allow extracting data to identify chilling damage with high precision [103]. On MODIS imagery, spatial interpolation was applied to minimum temperature data to acquire a spatially continuous image [104]. MODIS normalized difference vegetation index (NDVI) data were collected from satellite images covering Kansan and Ukraine cultivated lands [105]. In contrast, She et al. [78] used both MODIS and Chinese HJ-1A/B images for their study. Overall, satellite images provide information on a large scale, but the implementation and accuracy depend on the images' delivery time.

7.1.2.4. *Unmanned aerial vehicles (UAV)*.

Unmanned aerial vehicles (UAV) can be used to collect data in precision agriculture. Yuan and Choi [44] mounted an RGB and thermal camera on a DJI Matrice 600 Pro UAV to collect images from an apple orchard. The UAV flew at a nominated altitude to prevent blurry images. In 2019, Choudhury et al. [56] mounted a spectroradiometer and chlorophyll meter on a UAV to collect spectral and chlorophyll reflectance, respectively. Chen et al. [106] performed UAV flights at an altitude of 30 m above a wheat field. The UAV collected spectral reflectance through a MicaSence multispectral camera. Goswami et al. [47] flew a UAV over experimental fields of maize during the peak season to collect four-channel multispectral images. L´opez-Granados et al. [63] acquired UAV imagery to monitor almond flowering dynamics at field scale. Canopy reflectance was measured with a multispectral camera flown on a multi-rotor UAV over a wheat field [13].

7.2. *Data preparation*

Data preparation corresponds to cleaning and transforming the raw data before applying them to any analytical method.

Please cite this article as: S. Shammi, F. Sohel, D. Diepeveen et al., A survey of image-based computational learning techniques for frost detection in plants, Information Processing in Agriculture, https://doi.org/10.1016/j.inpa.2022.02.003

Raw data usually suffers from various nuisances, e.g. noise, blur, inconsistent illumination, affecting the results. Therefore, to obtain correct results, proper preparation and research design is a crucial step. This includes setting up the research design to enable the generation consistent images with minimal noise.

7.2.1. *Image enhancement*

In data preparation, image enhancement is one of the most important and complex techniques [107]. There are many image enhancement techniques such as colour conversion, contrast adjustment, thresholding, morphological operations used to make the image ready to apply any computational model [52,97].

7.2.1.1. Colour conversion. Fluorescence parameter images are usually one-dimensional grayscale images [67]. To facilitate the visualisation of the cooling phenomenon in tomato seedlings, they converted to RGB valued colour images [67,70]. However, converting to grayscale is commonly performed as image pre-processing [52,81,97].

7.2.1.2. Contrast enhancement. Contrast can enhance an image so that the pixels' colour properties are intensified from the neighbouring pixels. This process is adopted at the beginning of the image enhancement to make further processing easier[51,62]. After modifying the contrast of the image, the green colour of the healthy crop was enhanced [61].

7.2.2. *Noise removal*

Noise in an image can be defined as the random variation of colour or brightness information. It is produced by the sensor device, i.e., digital camera or circuitry of the scanner. Noise removal is a critical step for removing unnecessary information from the data. However, noises in an image can cause increased complexity resulting in increased false positives [62].

7.2.2.1. Filtering/smoothing. Filtering or smoothing is applied to remove noise from image data [17,60]. The atmospheric water absorption wave- lengths are removed from the spectra [49,60]. Weak spectral signals are removed to reduce the reflectance errors as well. Moreover, in their study, the Savitzky-Golay smoothing convolution was applied to smooth the reflectance curves [49,56,60]. Zhang et al. [52] excluded the noise wavelengths for better classification results. The global navigation satellite system (GNSS) module's images also contain noise. Median values are being used to remove this noise [44,55]. However, to remove the noise regions, mean spectra are calculated [17,50,97,108]. The pixel continuity determines noise reduction, excess green index, the ratio of blue/green, and red/green pixels [106]. Liu et al. [108] reconstructed a multi-phase NDVI time series using the Savitzky–Golay filtering. In contrast, Agelet et al. [58] used a smoothing method named Standard Normal Variate (SNV) to reduce the scattering effect. However, Macedo-Cruz et al. [61] averaged threshold values to smooth the spectral components.

7.2.2.2. Normalization. Normalization is another approach for noise removal [60]. Normalization is achieved by dividing the spectral data by the mean of reflectance [45,60,83]. Asante et al. [17] removed noise from the data within each image region by applying maximum normalization. The reflectance parameters were normalized using principal component analysis (PCA) to reduce the noise from multiple dimensions [50]. In the study of Macedo-Cruz et al. [61], they normalized the indexes of the three primary colours to generate tristimulus values relative to the white colour. In this study, they used the CIELab colour model. Jelowicki et al. [46] calculated the irradiance that was coming from the sun through the sunshine sensor included in a Sequoia camera. This feature enables them to normalize the images quickly. However, Perry et al. [13] normalized the spectra by continuum removal to reduce illumination artefacts from the spectral image.

7.2.3. *Region of interest (ROI)*

In a proximal or remote sensed image, there is considered unnecessary and redundant information, which leads to inaccurate prediction. A region of interest (ROI) is a portion of an image or data filtered to operate. For example, cropping is a basic image manipulation process to remove unwanted portions of an image [62,81].

7.2.3.1. Segmentation. Segmentation is partitioning an image based on objects or pixels [109,110]. For spectral images, calculating mean spectra in the spectral range are required to segment the border of the noise region [17]. A two-stage segmentation method was used by Ma et al. [81]. In their work, they followed coarse and fine segmentation with DCNN (Deep Convolutional Neural Network) and FCN (Fully Convolutional Networks). FCN allows pixel-wise semantic segmentation to remove the noise pixels. Segmentation can be based on thresholding, edge extraction, or morphological operation [111].

Thresholding is pixel-based segmentation [20,58,62,76], and probably the most straightforward method [111]. Otsu's method is a popular thresholding method for maximizing the variance of the black and white pixels. Otsu's method was used to scale the principal component score of the image [17,52,61]. Otsu's method was also applied to grey-scale images. Zhang et al. [52] applied the method at 500 nm, while Macedo-Cruz et al. [61] used the same method for a bi-class problem. Lu et al. [51] used an automatic threshold to achieve the best image contrast for plant segmentation.

Morphological operation is applied to segment images into smaller parts to enable further processing [51,61,80]. Morphological erosion was applied to the segmented images to eliminate areas that did not represent freeze injured tea leaves [17]. Enders et al. [80] detected edges of the plants by isolating only plant pixels. The pixels outside this boundary were excluded to facilitate the trait extraction.

7.2.3.2. Masking. Masking is a bitwise operation to set the background pixels to zero. With this operation, the pixels of the region of interest are identifiable. Masking was applied to the original hyperspectral images, and the average spectrum was applied to process the data before the analysis

Please cite this article as: S. Shammi, F. Sohel, D. Diepeveen et al., A survey of image-based computational learning techniques for frost detection in plants, Information Processing in Agriculture, https://doi.org/10.1016/j.inpa.2022.02.003

[80,83]. Cogato et al. [45] created masks with QGIS 2.4 (http://www.qgis.org/) for sentinel images to avoid border effects. In the study of Jelowicki et al. [46], the biggest challenge was identifying the roads and soil in the image. They applied a masking operation to subtract the road from the index rasters [45]. Enders et al. [80] applied masking to remove soil pixels from the plant pixels, which was important to measure the attributes of the cold stress in the plant.

7.2.3.3. *Image correction*. Images of different modalities require corrections before analysis. Usually, hyperspectral images come with white and dark references. So, the calibration of the hyperspectral image is calculated for correcting the raw images [17,55]. Fayad et al. [101] used calibrated Sentinel-1 image correction to covert pixel values into backscattering coefficients. A whiteboard approach was used for correction during measuring canopy hyperspectral reflectance [79]. Crop imagery was corrected for reflectance by using calibration panels at the canopy level [49,65]. However, Liu et al. [108] applied radiometric calibration, atmospheric correction, and geometric correction on satellite images. A similar approach was adopted by She et al. [78]. Becker-Reshef et al. [105] used BRDF-corrected MODIS reflectance imagery for their study.

7.2.3.4. *Indices generation*. The mathematical combinations of reflectance are generally calculated into spectral indices according to wavelength [60,102]. Wu et al. [60] extracted indices developed for chlorophyll-sensitive and water-sensitive stresses to predict yield loss in winter wheat. Eight vegetation indices are calculated based on Sentinel-2 data to describe the vegetation characteristics [20,75]. Murphy et al. [20] extracted vegetation-only pixels from the Red (656–670 nm), and Near Infrared (804–818 nm) regions. NDVI is one of the most commonly used indices for remote sensing of vegetation [20,78,79,100,105,108]. Liu et al. [108] compared NDVI values for different time phases of cultivated fields. However, Zhao et al. [104] assessed two-phase frost damage and showed the degree of damage by normalized vegetation indices. Gao et al. [55] generated a bud injury (BI) index for estimating the percentage of damage in flower buds. Feng et al. [50] calculated freeze-injury comprehensive evaluation index (FICEI) as an agronomic parameter. Twelve spectral indices that are correlated with frost damage and yield loss were measured by Perry et al. [65] In their study, they also used nine distinct fluorometer indices. Wei et al. [49] measured chlorophyll concentration indices from leaf spectra. They also discussed optimal band positions for each type of spectral vegetation index in their study. Mishra et al. [16] measured cold tolerance by generating parameters ChlF parameters: maximum quantum yield of PSII photochemistry (FV/FM) and fluorescence decrease ratio (RFD).

7.2.4. *Labelling*

Labelling is one of the most important steps of data preparation. This process can be very labour-intensive [81]. For proper characterisation or classifications, the data is tagged with one or more labels. Labelled data is beneficial for traditional machine learning and deep learning. Our study found that labelling can be pixel-wise, or it can be bounding boxes or logical arrays.

7.2.4.1. *Pixel-wise labelling*. There are various methods for pixel-wise labelling. Many researchers use pixel-wise labelling based on colour [16,63,68,72,78,90,99,104]. Different colour gradients were used as labels to classify the damage [52]. Cho et al. [82] labelled pixels according to three classes based on coefficients of variation, mean and standard variation of spectra. In comparison, Asante et al. [17] labelled the pixels as defective or non-defective and classified an image of a single grain when it contained more than five defective pixels. Dong et al. [70] also labelled the pixels into four categories depending on the cold injury level. In their work, they rejected the pixels that were less than their defined threshold value. Perry et al. [65] labelled pixels as frosted or non-frosted. The mean value of the indexes are assigned to the pixels [46]. NDVI values are labelled to individual pixels [13,78,84,100,103,105,106]. Goswami et al. [47] used labels to build the data set of four classes (healthy, stressed, weeds, non-cropped). Thermal image pixels are labelled with the corresponding temperature [43].

In the study by Yang et al. [53], a softmax function for the pooling layer of a convolutional neural network was used to output the classification label. Ma et al. [81] adopted a sampling strategy for the sub-images using image-labelling software to minimise the labour of labelling. Their data set consisted of 96 images with pixel labels. In unsupervised classification, a cluster labelling was done in an unsupervised classification on the RGB image by Macedo-Cruz et al. [61].

For MODIS images, pixels were labelled based on land surface temperatures [75,101,102]. Liu et al. [108] labelled 1 km pixels using the generalized split-window algorithm.

7.2.4.2. *Bounding box labelling*. Bounding box annotation defines the target object surrounded by a rectangular box. Yuan and Choi [44] labelled eight stages of apple flower by bounding boxes. The bounding boxes were different sizes depending on the bud stage. These annotations were prepared in Darknet format using YoloLabel (an open-source tool). HamidiSepehr et al. [62] used an image labeller to label images with bounding boxes for Faster R-CNN (Region-based Convolutional Neural Network) model. At the same time, they used a Matlab script and LabelImg software for preparing the labels for RetinaNet and YOLOv2 (You Only Look Once: version 2), respectively. On the other hand, bounding circles were drawn to discriminate between healthy and cold injured flowers [55].

7.2.4.3. *Logical array*. A logical array is a set of two classes inside the array that decide true or false. For instance, class labels are entered as a logical array, where each class is represented as a column of zeros or ones [58,59]. In this case, the two classes correspond to frost-damaged or healthy maize seeds [59]. In another study, Agelet et al. [58] also used similar labelling, where a threshold determined the class separation between frosted and sound corn kernels.

7.3. *Feature extraction*

For any computational approach, with the rise of data dimensionality, the complexity of the analysis also increases [86].

Please cite this article as: S. Shammi, F. Sohel, D. Diepeveen et al., A survey of image-based computational learning techniques for frost detection in plants, Information Processing in Agriculture, https://doi.org/10.1016/j.inpa.2022.02.003

Feature extraction is used to select the most useful data characteristics. The goal is to have a small number of features that preserve information for the data analysis [112].

7.3.1. Data dimensionality and redundancy reduction

Redundant information also increases the complexity of the analysis. The key to reducing data complexity is an accurate and efficient dimensionality reduction [113]. Principal component regression (PCR), partial least squares regression (PLSR) and linear model (LM) were examined to extract features [17,50]. PCR is a dimension reduction method that transforms highly correlated variables into uncorrelated principal components variables [114]. Partial least square regression (PLSR) decomposes the spectral information and response variables by using covariances [115], while a linear model (LM) can be used to estimate predictor variables [17]. Lu et al. [51] extracted spectral features from the reflectances in blue, red and NIR regions. These spectral features helped build models for freeze-induced damage and assessment [51]. Extraction of distinct spectral features is needed for hyperspectral image analysis [13,19,58].

In the study of Zhang et al. [83], principal component analysis (PCA), successive projection algorithm (SPA) and neighbourhood component analysis (NCA) were evaluated for extracting spectral features. PCA converts high dimensional data into a small set of comprehensive indicators by removing redundant information [116]. PCA is widely applied for extracting spectral information [54–56,117]. Jia et al. [59] used PCA and OLDA (orthogonal linear discriminant analysis) together to extract features from NIR spectra for normal and frost-damaged maize seeds. According to their study, OLDA was calculated from the extracted principal components to create an accurate model of extracted features. SPA removes redundant information and arranges the characteristic variables according to the size of correlation [118]. SPA is another popular method used for feature extraction [54,55]. However, NCA extracts features to achieve dimensionality reduction by measuring the Mahalanobis distance [119].

7.3.2. Keypoint descriptor

A keypoint descriptor is the point of interest in an image. A keypoint feature-based approach was used by Yuan and Choi [44]. In their study, they chose BRISK (Binary Robust Invariant Scalable Keypoints) over standard algorithms such as SIFT (scale-invariant feature transform) or SURF (Speeded up robust features). BRISK provides better accuracy and computational efficiency [120]. It identifies the image keypoints by comparing neighbouring image points in a binary manner [44]. In contrast, Mishra et al. [16] applied sequential forward floating selection (SFFS) to create a high-performing classifier.

7.3.3. Convolutional layers

In traditional machine learning, a feature map is required first, and then the classifier is applied. This process is sometimes complex because every set of data has diversity for different problems [121]. But in deep learning, convolutional layers can automatically generate the features from low-level to high-level layers according to their architecture [53,121]. Ma et al. [81] extracted low-level features for their shallow machine learning model. Resnet50, VGG16, and Darknet19 were chosen as feature extractors for Faster RCNN, RetinaNet, and YOLO [62]. In convolutional neural networks (CNNs), the layers continuously learn the input features [53,97]. The feature map passes through convolutional layers and the max-pooling layers to build the classifier [53].

7.3.4. Spatiotemporal pattern

From satellite imagery, the feature of frost damage depends on the spatiotemporal patterns. The changes in colour and texture on land cover over time can measure the minimum temperature variation in satellite image pixels [99,100]. Gobbett et al. [102] extracted variables from satellite data that are change factors depending on temperature and time. The temperature profiles over the land cover provide spatial matching between the experimental plots by utilising the nearest neighbour approach [101]. Liu et al. [75] have constructed a feature library with time, terrain, and vegetation features. She et al. [78] and Becker-Reshef et al. [105] evaluated spatial and temporal variations in surface features from MODIS images.

7.3.5. Phase change over time

Freezing happens when the temperature is below zero degrees over a period of time. In laboratory tests, after a freezing treatment, water inside plant tissues changes phase and forms ice [37,40,64,68]. This type of feature can be observed through visual inspection. The physical changes of plants are also a type of feature for following frost damage [68,117].

7.3.6. Other

In this section, we discuss several feature extraction methods that have been used but do not fit into any of the previous categories. Wu et al. [60] examined a coefficient of determination approach to select the best wavelengths having spectral features. However, from the green, red, red edge, and near-infrared spectral bands, three vegetation indices were chosen as features [46]. Murphy et al. [20] assessed mean spectral reflectance for target features. Colour based features are also a common method [51,61,72]. Another important feature selection is the Gini index, which can identify the best features by calculating the error based on misclassified pixels [47].

8. Computational methods used in image-based frost detection

Researchers investigated the freezing process in the early days by manual observation, were discussed in Section 3. More recently, computational methods have been developed that make frost detection and analysis more efficient. The first steps in the computational approach require data acquisition, preparation and feature extraction. In our review, we survey statistical, traditional machine learning and deep learning as computational methods.

8.1. Statistical analysis

A statistical analysis uncovers the patterns and trends in collected data. In our review, we found most of the articles used

Please cite this article as: S. Shammi, F. Sohel, D. Diepeveen et al., A survey of image-based computational learning techniques for frost detection in plants, Information Processing in Agriculture, https://doi.org/10.1016/j.inpa.2022.02.003

statistical analysis. For instance, mean, regression, hypothesis testing and descriptive statistics are most commonly used. In the sections below, we discuss the statistical methods adopted for frost detection in plants and crops.

8.1.1. Regression

Regression is a statistical approach to understand the relationship between variables. Wu et al. [60] evaluated the level of frost damage by predicting the percent yield difference (PYD). Their work selected nine vegetation indices on the best wavelength combination to establish a linear regression model. Their regression model showed significantly higher accuracy than partial least square regression (PLSR) and support vector regression (SVR) models. Similarly, to establish a quantitative evaluation of cold injury in tea plants, three regression models were compared [17]. Linear regression models outperformed the PLSR and principal component regression (PCR) to predict the cold injury. Feng et al. [50] observed the best performance for evaluating freeze stress in wheat with multiple linear regression (MLR). Feng et al. [50] compared five methods such as PCA, PLSR, correlation analysis, variable analysis and MLR to establish the freeze-stress prediction model.

Linear regression was used to predict the yield reduction in field crops [12,19,49,72,79]. Xie et al. [79] applied MLR to explore the effect of low-temperature stress in winter wheat. They evaluated the relationship between spectral reflectance and the yield of winter wheat. Their model showed better performance than SPA in predicting crop yield. Fitzgerald et al. [19] quantified the frost damage with linear regression models. Wei et al. [49] discussed the findings by applying MLR for automatic detection and monitoring of freezing injury in oilseed rape leaves. They assessed the physiological status and yield loss by investigating the vegetation indices through their model. Regression-based cold-sum based on the indices was used for predicting wheat yield loss [13], where a cold sum is a product of negative temperature and the duration of the freezing event.

Cho et al. [82] compared satellite-derived regression models with field-based models to test the dependency of temperature and satellite phenology. They explored the patterns and factors that control the thermal parameters of the canopy by regression analysis. Gobbett et al. [102] also applied Multivariate Adaptive Regression Splines (MARS) on high-resolution MODIS data. They observed the relationship between nighttime temperature and its impact on current and future frost risk in grapevines. Kotikot et al. [90] statistically characterised some known topographical risk factors such as elevation, convexity, aspect and land surface temperature through a binary logistic regression in the Kenyan highlands. Becker-Reshef et al. [105] evaluated a regression model on MODIS images to forecast winter wheat production due to frost events.

Lu et al. [51] studied freeze-induced damage and prediction in loblolly pine seedlings with a regression model. They assessed the freeze-induced damage from hyperspectral imaging combined with some chemometric techniques. They observed a significant relationship between the minimum winter temperature and freeze damage. Arnold et al. [68] described a linear model for characterising plant function with response to minimum temperature.

8.1.2. Hypothesis test

Analysis of variance (ANOVA) and Student *t*-test are statistical methods for observing the relationship or comparison in two or more groups [122]. The Student *t*-test observed statistical significance to assess frost [20,45,117]. To do so, they observed the relationship between spectral reflectance and numerous vegetation indices.

The correlation between cold sensitivity and genotypes was shown by ANOVA [42,80]. Choudhury et al. [56] also developed the hypothesis for chlorophyll absorption index with spectra taken after frost. A significance test was used along with object-based image analysis to observe better the monitoring of flower density [63]. Kimball et al. [64] applied ANOVA across four freezing temperatures on St. Augustinegrass to observe the response. In 2016, Livingston III et al. [35] also investigated freezing patterns in different wheat genotypes using ANOVA (standard F-tests and Tukey-Kramer mean separation tests).

8.1.3. Descriptive statistics

Descriptive statistics are used to summarise the features of the data [123]. Mean and Standard Deviation (SD) is used in many research works for frost analysis [16,57,70,106,108]. Dong et al. [70] calculated the mean and SD on grey-scale co-occurrence to evaluate chilling damage in tomato seedlings. Liu et al. [108] established a threshold model for frost detection by taking the mean value of time.

8.1.4. Time-series analysis

Time-series analysis of thermal data is a popular method to investigate the freezing behaviour in plants [42]. Stegner et al. [38] studied the freezing process in potato leaves by employing infrared differential thermal analysis (IDTA). This process clarifies freezing behaviour by explaining the relationship between frost injury and ice propagation [36,38,39,66]. Neuner [22] observed the freezing process in vegetative buds by using IDTA. This process enhanced the ability to visualise ice nucleation and propagation. Kokin et al. [43] used time series analysis to see how the strawberry leaf surface temperature varied in night frost conditions. Frost susceptibility in blackberry crowns was determined by measuring the exotherm with IDTA [124].

8.2. Traditional machine learning

Traditional machine learning algorithms such as support vector machines (SVMs) are mature enough to be applied to images [125]. However, there is still room for improvement. In the articles reviewed, most of the researchers applied SVMs as traditional machine learning algorithm [47,52,54,91,97]. This is one of the best general classifiers in traditional machine learning [126]. In this section, we review few traditional ML algorithms that have been used for frost detection in plants.

8.2.1. Support vector machine

A Support Vector Machine (SVM) [127] is a traditional machine learning method that is now often used because of its simplicity and flexibility for addressing a range of classification

Please cite this article as: S. Shammi, F. Sohel, D. Diepeveen et al., A survey of image-based computational learning techniques for frost detection in plants, Information Processing in Agriculture, https://doi.org/10.1016/j.inpa.2022.02.003

Table 2 – Evaluation metrics used in frost detection models.

Method	Evaluation metric	Definition and interpretation	Sample references where used
Statisticalanalysis	R^2	It gives the percent variation between variables.$0 \leq R^2 \leq 1$Higher value indicates better model.	[60,82,17,68,102,104,12,19,90,50,72,106,49,13,105].
	$p-$ value	It is used to find the significance level.$0 < p-$ value $< 1p > 0.05$, null hypothesis is true;$p \leq 0.05$, test hypothesis is false;$p > 0.05$, no effect was observed.	[60,82,51,65,117,56,64,66,45,80,20,42,103,36].
	RMSE	It is basically prediction error.$0 <$ RMSE $< 10.2 <$ RMSE < 0.5, good prediction;RMSE ≥ 0.5, poor prediction; Lower value indicates better performance.	[17,102,49].
TraditionalMachinelearning/ Deeplearning	Confusion matrix	It is a table consisting true positives, false positives, true negatives and false negatives.	[75,97,59,55,99,61,53,83,91,47].
	Kappa coefficient	$K \leq 1.1$ indicates best performance.	[75,47,91].
	F1-score	It is weighted from precision and recall.$0 \leq F1 - score \leq 1$Higher value indicates better prediction.	[46].
	Intersection over union (IoU)	It is measured from ground truth and prediction boxes.$0 \leq IoU \leq 1IoU > 0.5$ indicates good performance.	[44].
	Mean average precision (mAP)	$0 <$ mAP < 100Higher value means better accuracy.	[44,53].

Please cite this article as: S. Shammi, F. Sohel, D. Diepeveen et al., A survey of image-based computational learning techniques for frost detection in plants, Information Processing in Agriculture, https://doi.org/10.1016/j.inpa.2022.02.003

Table 3 – An overview of different image based computational approaches for frost detection and analysis. Note: a hyphen (-) indicates the attribute was not explicitly mentioned in the respective paper.

Ref.	Crop	Application	Data Type	Data Set Size	Remote/ Proximal	eature Type	Method	ML/DL/ Statistical Model	Techniques Applied (based on Taxonomy)
[60]	Wheat	Predicting percent yield difference of frost damaged crop	Narrow waveband	77–112	Proximal	Spectral features	Statistical Analysis	PLSR, SVR	CE; (S, N, IG, PW); R.
[75]	Grape	Assessing risk of late frost	Multispectral	90	Remote	Vegetation Index	Traditional Machine Learning	RF	S; (IG, PW); STP; RF.
[44]	Apple	Frost management	Thermal, RGB	100, 6 120	Remote	Temperature map	Deep Learning	YOLOv4	UAV; (F, BB); Ked; CNN.
[82]	Subtropical forest	Assessing chilling adaption	Spectral Reflectance (MODIS)	–	Remote	NDVI	Statistical Analysis	LR	S; (IG, PW); STP; R.
[17]	Tea	Assessing nitrogen effect on cold tolerance	Hyperspectral	24, 30	Proximal	Spectral features	Statistical Analysis	PLSR, PCR, LM	CE; (S, N, Sg, IC, PW); DDRR; R.
[142]	Periwinkle	Detecting cold stress	Fluorescence	–	Proximal	Colour	Statistical Analysis	Non-linear Regression	CE; (IG, PW); STP; R.
[51]	Loblolly pine	Predicting frost damage	Hyperspectral	–	Proximal	Temperature, Spectral	Statistical Analysis	SPA-PLS	CE; (CEn, Sg, IC, PW); DDRR; R.
[72]	Rose	Evaluating freezing resistance	Electrical impedance tomography	1 680	Proximal	Temperature	Statistical Analysis	LR	CE; (IG, PW); O; R.
[97]	Corn	Identifying freeze damage degree	Hyperspectral	1 920	Proximal	Spectral feature	Deep Learning, Traditional MachineLearning	DCNN, SVM, K- NN, ELM	CE; (CC, S, Sg, IC, PW); CL; (SVM, K-NN); CNN.
[68]	Lothian waxy bluebell, Willow oak, Curtis and Myretaceaebottlebrush	Assessing response to minimum temperature	Chlorophyll Fluorescence	–	Proximal	Temperature dependent changes	Statistical Analysis	LR	CE; PW; PCoT; R.
[90]	Tea	Characterising frost prone zones	Spectral Reflectance (MODIS)	282	Remote	Spatiotemporalpattern	StatisticalAnalysis	Significance test	S; PW; STP; R.
[83]	Rice	Classifying frost damaged seeds	Hyperspectral	1 800	Proximal	Spectral features	Deep Learning, Traditional Machine Learning	DF, DT, K-NN, SVM	CE; (S, N, Sg, M, IC, PW); (DDRR, CL); (SVM, K-NN, DF).
[102]	Grapevine	Managing frost risk	Spectral Reflectance (Landsat)	–	Remote	NDVI	Statistical Analysis	MARS Model	S; (IG, PW); STP; R.
[67]	Tomato seedling	Analysis of chilling injury	Chlorophyll Fluorescence	220	Proximal	Chlorophyll Fluorescence, Parameter value, Histogram, Texture, Colour descriptor	Traditional Machine Learning	BPNN	CE; (CC, M, IC, PW); O; O.
[117]	Arabidopsisthaliana	Analysing repair of freeze damage	Chlorophyll Fluorescence	–	Proximal	Temperature dependent changes	StatisticalAnalysis	Significance test	CE; PCoT; HT.
[62]	Corn	Detecting frost damage	RGB	470	Remote	Colour	Deep Learning	YOLOv2, RetinaNet, Faster R-CNN	UAV; (CC, Sg, BB); CL; CNN.
[45]	Vineyard	Assessing frost damaged vineyards	Multispectral(Sentinel)	2	Remote	Spectral	StatisticalAnalysis	Student's *t* test	S; (CEn, N, M, IG, PW); HT.
[46]	Rapeseed	Detecting frost damaged area	Multispectral	–	Remote	Spectral	StatisticalAnalysis	OBIA, SD	UAV; (N, M, PW); O;
[57]	Wheat, Barley	Assessing frost damage	Terahertz	–	Proximal	Phenological difference	StatisticalAnalysis	SD	CE; PW; DS.
[20]	Wheat	Detecting frost stress	Hyperspectral	1 000	Proximal	Spectral	StatisticalAnalysis	Student's *t*-test	CE; (IG, PW); O; HT.
[76]	Corn	Identifying frostbite condition in seeds	Hyperspectral	–	Proximal	Spectral features	Traditional MachineLearning	SVM	CE; (S, Sg, IC, PW); O; SVM.
[54]	Wheat	Classification of frost damaged kernel	Hyperspectral	720	Proximal	Colour, Morphological	Traditional MachineLearning	LS-SVM	CE; (IC, PW); DDRR; SVM.
[101]	Cropland	Detecting frost in real-time	Spectral Reflectance	133,154	Remote	STP	StatisticalAnalysis	Quantitative Analysis	S; (IC, PW); STP; HT.
[104]	Wheat	Monitoring winter frost damage	Spectral reflectance	210	Remote	Frost duration, Temperature, NDVI, Frost continuity	Traditional Machine Learning	Regression, RF	S;(IC, IG, PW); R.
[135]	Loblolly pine	Assessing freeze tolerance	Hyperspectral	1 549	Proximal	Spectral	Traditional MachineLearning	SVM	CE; (IC, PW); O; SVM.
[79]	Wheat	Evaluating freezing injury	Hyperspectral	–	Proximal	Spectral	StatisticalAnalysis	MLR, PCR, SPA-MLR	HH; (IC, IG, PW); DDRR; R.
[81]	Wheat	Segmenting frost-damaged spikes	RGB	24 000,34 520	Proximal	Colour	DeepLearning	DCNN, FCN	MP; (CC, Sg, M, PW); CL; CNN.
[73]	Common box, Snowdrop,Norway spruce	Observing ice nucleation	Reflected polarised light	–	Proximal	State	Statistical Analysis	–	CE; PCoT.
[108]	Cultivated land	Monitoring frost disaster onland cover	Spectral reflectance	240	Remote	Landscape feature	StatisticalAnalysis	STP analysis	S; (F, PW); DDRR; DS.
[55]	Blueberry	Frost damaged floral bud detection	Hyperspectral	390,360	Proximal	Phenological difference, Spectral	TraditionalMachine Learning	PLS-DA	CE; (S, IC, IG, BB); DDRR; O.

Please cite this article as: S. Shammi, F. Sohel, D. Diepeveen et al., A survey of image-based computational learning techniques for frost detection in plants, Information Processing in Agriculture, https://doi.org/10.1016/j.inpa.2022.02.003

Table 3 – (*continued*)

Ref.	Crop	Application	Data Type	Data Set Size	Remote/ Proximal	eature Type	Method	ML/DL/ Statistical Model	Techniques Applied (based on Taxonomy)
[80]	Maize	Cold Stress Analysis	RGB	4	Remote	Morphological	StatisticalAnalysis	ANOVA, Post-hocTukey HSD	CE; (S, Sg, M, PW); HT.
[53]	Corn	Cold/frost damage prediction	Hyperspectral	3 600	Proximal	Abstract, Invariant	DeepLearning	CNN	CE;(F, Sg, IC, PW); CL; CNN.
[56]	Maize	Assessing frost damage	Hyperspectral, RGB	–	Remote	Spectral	StatisticalAnalysis	Regression	UAV; (S, IG, PW); DDRR; R.
[106]	Wheat	Analysing winter survival strategy	Multispectral	–	Remote	Phenotyping features	StatisticalAnalysis	LM	UAV; (IC, IG, PW); O; DS.
[47]	Maize	Frost affected area identification	Multispectral	964,1 017	Remote	Spectral	TraditionalMachine Learning	SVM, ANN, RF, RC	UAV; (N, PW); O; (SVM, RF, O).
[77]	Maize	Examining the yield due to frost	Spectral reflectance	–	Remote	Landscape feature	Traditional MachineLearning	ANN;	S; (IC, IG, PW); O; O.
[63]	Almond	Reducing risk of late frost	RGB	–	Remote	Colour	StatisticalAnalysis	Tukey HSD	UAV; PW; HT.
[38]	Potato leaf	Freezing process analysis	Thermal	–	Proximal	SpatiotemporalPattern	StatisticalAnalysis	IDTA	CE; PCoT; TA.
[52]	Corn	Classification of frozen seeds	Hyperspectral	180, 180, 144	Proximal	Spectral	Traditional MachineLearning	SVM, K-NN, PLS- DA	CE;(S, Sg, PW); DDRR; (SVM, K-NN, O).
[12]	Wheat	Frost damage assessment	Spectral, Fluorescence	40	Proximal	Spectral	StatisticalAnalysis	Correlation,ANOVA, LR	H; (IG, PW); O; (HT, DS, R).
[70]	Tomato	Diagnosis of chilling injury	Chlorophyll fluorescence	220	Proximal	Heterogeneity, Histogram, Texture	StatisticalAnalysis	Mean, HistogramDistribution	CE; (IC, PW); DS.
[143]	Oilseed rape	Assessing freezing damage degree	Spectral reflectance (MODIS, MERIS)	–	Remote	NDVI, landscape	StatisticalAnalysis	Correlation	S; (IG, IC, PW); O; DS.
[19]	Wheat	Frost damage assessment	Hyperspectral	31	Proximal	Spectral	StatisticalAnalysis	Regression	CE; (IG, PW); DDRR; R.
[41]	Alnus alnobetula	Assessing freezing and ice nucleation	Thermal	10	Proximal	Ice nucleation temperature	StatisticalAnalysis	IDTA	CE; TA.
[144]	Peach flower	Assessing low temperature damage	Fluorescence	80	Proximal	External structure	StatisticalAnalysis	–	CE; PCoT.
[91]	Common beech	Assessing spring frost effects	Spectral reflectance	–	Remote	Phenological homogeneity	Traditional MachineLearning	SVM	S; (N, PW); O; SVM.
[43]	Strawberryleaf	Observing frost dynamics	Thermal	8 140–12 539	Proximal	Temperature	StatisticalAnalysis	DTA	MP; PW; TA.
[84]	Canola	Frost damage estimation	Hyperspectral	–	Proximal	Spectral	StatisticalAnalysis	ANOVA	CE; (S, Sg, IC, IG, PW); HT.
[40]	Wheat	Observing ice nucleation and propagation	Thermal	–	Proximal	State	StatisticalAnalysis	–	CE; PCoT.
[42]	Arabidopsisthaliana	Analysing frost resistance	Thermal	–	Proximal	Ice nucleating temperature	StatisticalAnalysis	–	CE; PCoT.
[136]	Tea	Identification of frost damage	Spectral reflectance (MODIS)	41	Remote	Landscape feature	MachineLearning	SLR	S; (IG, PW); R.
[145]	Beech forest	Assessing the effect of latespring frost	Spectral reflectance (MODIS)	–	Remote	NDVI	StatisticalAnalysis	STP variability analysis	S; (N, M, IC, IG); STP.
[50]	Wheat	Monitoring freeze stress	Hyperspectral	87	Proximal	Spectral	StatisticalAnalysis	MLR, Correlation	MP; (S, N, IG, PW); DDRR; (R, HT).
[65]	Wheat	Detecting frost damage early	Multispectral, Fluorescence	62	Proximal	–	StatisticalAnalysis	ANOVA	H; (N, IG, PW); O; HT.
[103]	Rice	Identifying chilling damage	Spectral reflectance (MODIS, Landsat)	–	Remote	Colour, landscape	StatisticalAnalysis	Comparison	S; (N, PW); STP; DS.
[64]	St. Augustinegrass	Assessing freezing tolerance	RGB	–	Proximal	Green colour	StatisticalAnalysis	ANOVA	CE; STP; HT.

Continued next page

Table 3 – continued from previous page

Ref.	Crop	Application	Data Type	DataSet Size	Remote/Proximal	Feature Type	Method	ML/DL/ StatisticalModel	Techniques Applied (basedon Taxonomy)
[49]	Oilseed rape	Characterising freezing injury	Hyperspectral	26	Proximal	Spectral	StatisticalAnalysis	PCA, ILR, SVM,SDR	CE; (S, IG, PW); DDRR; R.
[13]	Wheat	Detecting frost damage	Hyperspectral	44	Remote	Spectral	StatisticalAnalysis	Regression	UAV; (IG, PW); R.
[129]	Oilseed rape	Assessing freeze injury	Spectral reflectance (MODIS, MERIS)	–	Remote	NDVI	StatisticalAnalysis	Time-series analysis, Correlation	S; (S, N, IC, IG, PW); STP; (DS, TA).
[59]	Maize	Analysing frost damaged and non-viable seed	NIR Spectral	400	Proximal	Spectral	Traditional MachineLearning	SVM, BPR, MD	CE; LA; DDRR; (SVM, O).
[124]	Blackberryflower	Evaluating freeze damage	Thermal	–	Proximal	Exotherm	StatisticalAnalysis	Time Series Analysis	CE; TA.
[35]	Wheat	Analysing freeze tolerance in different genotypes	Infrared thermal	–	Proximal	Exotherm	Statistical Analysis	ANOVA,Standard F-Test, Tukey-Kramer separation	CE; PCoT; HT.

(*continued on next page*)

Please cite this article as: S. Shammi, F. Sohel, D. Diepeveen et al., A survey of image-based computational learning techniques for frost detection in plants, Information Processing in Agriculture, https://doi.org/10.1016/j.inpa.2022.02.003

Table 3 – (*continued*)

Ref.	Crop	Application	Data Type	Data Set Size	Remote/ Proximal	eature Type	Method	ML/DL/ Statistical Model	Techniques Applied (based on Taxonomy)
[78]	Oilseed rape	Assessing freeze injury	Multispectral	–	Remote	Landscape, NDVI	StatisticalAnalysis	Correlation	S; (IG, IC, PW); HT.
[48]	Wheat	Investigating freezing susceptibility	Hyperspectral	70	Remote	Spectral	StatisticalAnalysis	ANOVA	CE;(IC, IG, PW); HT.
[146]	Cropland	Evaluating spectral indices with frost	RGB	–	Proximal	Colour	StatisticalAnalysis	Regression	MP; (F, IG, PW); STP; R.
[99]	Kenyan highlands	Frost risk assessment	Spectral reflectance (MODIS, LST)	–	Remote	Landscape	StatisticalAnalysis	Time series analysis	S; STP; TA.
[147]	Grapevine	Evaluating frost tolerance	Chlorophyll fluorescence	–	Proximal	Electrolyte leakage	StatisticalAnalysis	Significance test	CE; (IC, PW); STP; HT.
[39]	Blueberry	Assessing freeze tolerance and ice nucleation	Infrared thermal	–	Proximal	Ice nucleation temperature	StatisticalAnalysis	IDTA	CE; TA.
[22]	Buds of woodyplants	Analysing freezing and ice tolerance	Thermal	–	Proximal	–	StatisticalAnalysis	IDTA	CE; TA.
[16]	Arabidopsisthaliana	Analysing cold acclimation	Chlorophyll fluorescence	218	Proximal	Cold tolerance	StatisticalAnalysis	LDA, LDC, QDC,k-NNC, NMC	CE; (IG, PW); DDRR; HT.
[66]	Wheat, Oats	Assessing recovery from freezing	RGB	100–300	Proximal	Colour	StatisticalAnalysis	Tukeys HSD	CE; O; HT.
[36]	Wheat	Observing cold acclimation and freezing	Infrared Thermal	29–88	Proximal	Exotherm	StatisticalAnalysis	DTA	CE; TA.
[148]	Wheat	Monitoring freeze stress in seedlings	Hyperspectral	30	Proximal	Index variation	StatisticalAnalysis	Correlation	CE; (IC, IG, PW); DS.
[149]	Wheat	Assessing freezing injury	Hyperspectral	44	Proximal	Spectral	StatisticalAnalysis	Correlation	CE; (IC, PW); HT.
[58]	Soybean, Corn	Classifying frost damaged kernel	NIR Spectral	504,480	Proximal	Spectral	Traditional MachineLearning	PLS-DA,K-NN, LS-SVM, SIMCA	CE; (S, LA); DDRR; (SVM, K-NN, O).
[61]	Oats	Classifying healthy and frost damaged area	RGB	2 000	Proximal	Colour	Traditional MachineLearning	K-means clustering	MP; (CC, S, PW); O; U.
[37]	Alpine cushionplants	Investigating freezing pattern	Infrared thermal	–	Proximal	Ice nucleation temperature	StatisticalAnalysis	IDTA, Correlation	CE; STP; (TA, DS).
[71]	Arabidopsis thaliana	Assessing cold tolerance	Chlorophyll fluorescence	325	Proximal	Electrolyte leakage	StatisticalAnalysis	LDA	CE; PCoT.
[100]	Aspen	Predicting defoliation due to frost	Spectral reflectance (MODIS)	–	Remote	NDVI	StatisticalAnalysis	SD	S; (IG, PW); STP; HT.
[105]	Wheat	Forecasting yield due to frost	Spectral reflectance	–	Remote	NDVI	StatisticalAnalysis	Regression	S; (IG, PW); O; R.

Please cite this article as: S. Shammi, F. Sohel, D. Diepeveen et al., A survey of image-based computational learning techniques for frost detection in plants, Information Processing in Agriculture, https://doi.org/10.1016/j.inpa.2022.02.003

problems [128]. The main advantage of SVM is that it is simple, computationally less expensive and, can be trained with a small number of samples [127]. However, selecting the optimal kernel and its parameters is the biggest challenge [47]. In crop stress classification, SVM has been widely used. Zhang et al. [83] applied SVMs on hyperspectral imaging to discriminate rice seeds for different degrees of damage. In their study, they compared other ML methods with SVMs to visualise the most rapid classification. In another similar study, Zhang et al. [97] compared four traditional ML models, including SVMs, to measure corn seed freezing. In this case, the deep learning model outperformed other traditional ML models. In another study, Zhang et al. [52] showed the comparison among ML models. Jia et al. [59] applied three ML models to see their performance for analysing frost-damaged maize seeds. In their study, SVMs showed promising results to discriminate between two classes.

Bascietto et al. [91] trained an SVM classifier on each pixel of remotely sensed data to assess spring frost effects in a beech forest. They assessed spring frost damage by using anomaly detection on each pixel corresponding to an enhanced vegetation index. After the data preparation, the SVM is used for training the model to classify two cases [47]. Their study demonstrated that the classifier could identify stress-free and stressed (before and after frost) maize crops from remotely sensed hyperspectral data.

Agelet et al. [58] utilised the least square support vector machine (LS-SVM) for corn kernel and soybean frost- damage classification. However, their study shows that frost-damaged corn kernels could not be accurately identified with LS-SVM with data from near-infrared spectroscopy.

8.2.2. *K-nearest neighbours*

The K-NN algorithm makes classification decisions based on the majority of the k-neighbouring samples in a feature space of a specific category [129]. Zhang et al. [52] showed that the classification results were similar with both K-NN and SVM. In a similar study by Zhang et al. [97], K-NN showed poor classification accuracy for the freezing damage degree of corn seeds. Agelet et al. [58] used standard normal variate to decrease the misclassification rate. Despite doing that, K-NN could not show satisfactory results comparing to PLS-DA.

8.2.3. *Random forest (RF)*

Random forest is an ML technique where many decision trees are generated, and the class is elected by a voting process [130]. Usually, the performance of the RF depends on the optimal number of a decision tree. Liu et al. [75] applied random forest classification on sentinel images to assess the late frost risk on the open-air grape parcel. In their work, they trained the RF model based on their proposed feature library. Their model showed high accuracy when 200 trees were selected. Zhang et al. [83] applied a cascaded RF model that contained 500 trees as their deep forest model base. According to Zhao et al. [104], a random forest regression analysis was conducted based on NNVAI and seven other features. This model showed a satisfactory correlation between NNVAI and frost severity in almost real-time. In 2019, Goswami et al. [47] built an RF model with a base of 100 decision trees.

8.2.4. *Others*

Zhang et al. [97] applied extreme machine learning (ELM) for analysing seed freezing damage. ELM is a single hidden layer feed-forward neural network that has good computational speed. Though it showed good performance, it still was not the best among the four models evaluated. On the other hand, Goswami et al. [47] employed three hidden layers to realise with back-propagation techniques to train an ANN model. They achieved moderate accuracy for the classification.

Goswami et al. [47] applied discriminant models for classifying normal and frost injured buds. Partial least square discriminant analysis (PLS-DA) was used to find a linear relationship between dependent and independent variables. In this study, Gao et al. [55] revealed their model depicted optimal performance with sensitivity and specificity. PLS-DA had higher accuracy than traditional SVM and K-NN models [52]. Mahalanobis distance discriminant analysis was used to assess frost-damaged maize for seed vigour, and viability [59].

Macedo-Cruz et al. [61] applied an unsupervised approach for frost-damaged oat-crop classification. Their study proposed a new automatic unsupervised classifier to identify frost-damaged oat-crop from the land area. Their methodology included a variable number of clusters to identify four classes.

8.3. *Deep learning*

Recently, some deep learning algorithm has been evaluated for frost detection in crops. Yuan and Choi [44] used YOLOv4 (You Only Look Once: version 4) for classifying six apple flower-bud growth stages as a measure of frost protection. YOLOv4 is currently the state-of-the-art real-time object recognition algorithm [131]. Yuan and Choi [44] performed the model training, validation, and testing on the annotated images. Their study also included a heating methodology for proper frost protection. HamidiSepehr et al. [62] trained and tested Faster R-CNN models, RetinaNet and YOLOv2 models to evaluate the performance for frost damage assessment. Both YOLOv2 and RetinaNet demonstrated robust capability to identify the frost-damage.

Zhang et al. [83] analysed the performance of a deep forest (DF) model with some traditional machine learning models such as decision tree (DT), K-NN, and SVM for classifying frost-damaged rice seeds. They reported that the accuracy of the DF model was superior to the other models in a small-scale sample set. Similarly, Zhang et al. [97] compared the performance of four models, namely K-NN, SVM, extreme learning machine (ELM) and deep convolutional neural network (DCNN), to classify the different freeze-damage of corn seeds. In their five-category classification, the DCNN outperformed all the other methods.

9. Evaluation metrics

An evaluation metric is a tool to measure the performance of a classification model. Our review discusses the relevant metrics for the three different computational learning methods,

Please cite this article as: S. Shammi, F. Sohel, D. Diepeveen et al., A survey of image-based computational learning techniques for frost detection in plants, Information Processing in Agriculture, https://doi.org/10.1016/j.inpa.2022.02.003

i.e., statistical, machine learning, and deep learning. There is no unified quantitative metric that consistently reproduces the overall performance score in all aspects. In general, no single metric outperforms all other techniques from an analytical viewpoint. As such, a single evaluation metric is not adequate to evaluate the performance. Therefore, several evaluation metrics are commonly used in literature. In Table 2, we summarise some standard evaluation metrics used in the reviewed publications.

In statistical analysis, coefficient of determination (R^2) and p-value are commonly used [132]. The coefficient of determination gives the variation in the dependent variable that is predictable from the independent variables. R^2 is represented as a value from 0.0 to 1.0. A higher (R^2) value indicates a better fit for a model. On the other hand, a p-value is used to find the smallest significance level to reject the null hypothesis. A smaller p-value indicates stronger evidence of the alternative hypothesis. A higher than 0.05P-value (>0.05) shows strong evidence for the null hypothesis (i.e., statistically insignificant). The p-value is usually used in statistical hypothesis testing. Another important evaluation metric is a root mean square error (RMSE), commonly used in regression models. RMSE is calculated based on the best fit line where the highest concentration of data is found. It is calculated by the square root of the mean square error. A lower value of RMSE reflects the better ability of the model to predict the data accurately.

In both ML and DL, confusion matrix, F1-score, precision and recall are commonly used to evaluate the performance. The confusion matrix allows visualization of the performance of a model. For a two-class model, this table consists of true positives, false positives, true negatives and false negatives [133]. From a confusion matrix, five different metrics can be calculated, e.g. accuracy, misclassification, precision, recall (sensitivity), and specificity [134]. A higher value of accuracy that is close to 1.0 is interpreted as a better classification. F1-score is calculated from precision and recall, where the highest possible value of an F1-score is 1.0 (i.e. indicates perfect precision and recall). On the other hand, a lower value of the Kappa-coefficient indicates a better agreement between the two raters. Unlike binary classifiers, for a multi-class model, each row of confusion the matrix represents the instances of an actual class, whereas each column represents the instances of a predicted class or vice versa.

In deep learning, we note the use of intersection over union (IoU) and mean average precision (mAP) as an evaluation metric. IoU quantifies the percentage of overlap between the prediction and target mask. Usually, IoU > 0.5 is considered a good prediction. An mAP is calculated by taking the mean of the average precision on all particular object classes. On the other hand, mAP computes the average precision value for recall as a value over 0 to 1.

The reviewed papers use different data sets (usually collected independently) as well as a variety of training and testing protocols. As a result, a direct comparison between the reported results is not feasible. In addition to performance (e.g., accuracy), the requirement of advanced computational resources are major concerns for computational learning models. Training on large and high-resolution data sets are usually computationally expensive. Yet deep learning techniques generally achieve superior performance compared to traditional machine learning techniques for image-based frost detection. Yuan and Choi [44] applied YOLOv4 and achieved 71.57% mAP for a test data set of 360 images. They used NVIDIA GeForce RTX 2060 (USA) GPU and 16 GB RAM to execute the training. Ma et al. [81] used NVIDIA Quadro P4000 (8 GB memory) with CUDA 9.0 to train a large data set of 19 199 and 23 775 images and achieved 92.15% accuracy for fine segmentation. Zhang et al. [97] compared accuracies of KNN, SVM, ELM, and DCNN models to classify damages in corn with Spyder 3.1.4 (Anaconda, Austin, TX, USA). The accuracies on the validation set are 95.3%, 99.7%, 98.4%, and 100%, respectively. In another study, RetinaNet and YOLOv2 were used by Hamidisepehr et al. [62] to distinguish the extent of damage in corn, with AP ranging from 98.43% to 73.24% and from 97.0% to 55.99%, respectively. They executed the models with NVIDIA Tesla P100 and NVIDIA Ge-Force GTX 1080 GPUs and empirically determined the learning rate, batch size, epoch number to minimise the training time and achieve higher accuracy. Zhang et al. [83] executed DT, K-NN, SVM and deep forest (DF) models with Spyder 3.3.2 to classify 300 rice seeds with different degrees of frost damage, and overall accuracy reached 99.33% for DF classification. Jia et al. [59] applied SVM, BPR and MD, and BPR achieved the highest average accuracy of 97% in classifying normal and frost-damaged seeds. In the study of Zhang et al. [52], the SPA wavelength selection method increased the accuracy of classification models to over 90% for classifying frozen corn seeds. Goswami et al. [47] achieved an overall accuracy of 86.47% by RF that outperformed other traditional machine learning techniques such as RC and SVM. Macedo-Cruz et al. [61] classified healthy and frost-damaged oat crops by K-means clustering with 90–97% accuracy. Several studies incorporate other statistical analyses, which are not comparable with these results. Furthermore, all the aforementioned accuracies and training resources are based on specific crops, evaluation metrics and different locally generated data sets and therefore, are not directly comparable. These resources are especially utilised by tuning hyperparameters such as batch size, the number of epochs, learning rate to reduce the long training time and increase accuracy. Deep learning models require powerful GPUs and a longer time for training compared to traditional machine learning. In contrast, deep learning techniques are usually computationally efficient in the testing phase, and they usually achieve higher accuracy compared to traditional machine learning techniques.

10. Data sets

Data sets are crucial for computational techniques, especially for machine learning and deep learning models. In general, publicly available benchmark data sets are used in typical machine learning research. In contrast, there is no benchmark data set available on frost detection. Moreover, the papers we reviewed mainly used small data sets that are crop and farm specific, and were collected locally by the respective research teams.

In Table 3, we summarise the data set size used in these papers. For example, Yuan and Choi [44] tested a deep learning model on 100 thermal images and 6 120 RGB images.

Please cite this article as: S. Shammi, F. Sohel, D. Diepeveen et al., A survey of image-based computational learning techniques for frost detection in plants, Information Processing in Agriculture, https://doi.org/10.1016/j.inpa.2022.02.003

Zhang et al. [97] created a data set of 1 920 images to apply several traditional machine learning algorithms. Similarly, others also applied deep learning and traditional machine learning techniques on relatively small data sets. For example, data sets of 1 800, 220, 478, 720, 210, 1 549, 3 600 samples were used in [53,54,62,67,83,104,135], respectively. Ma et al. [81] used a relatively large data set of 24 000 images of wheat ears. Yet, they applied data augmentation to generate a larger data set of 34 520 images. In contrast, Gao et al. [55] constructed a data set of 360 and 390 images in different categories. Zhang et al. [52] used 180 images in the data set. In the study of Goswami et al. [47], and Jia et al. [59], they applied traditional machine learning classifiers on spectral image data sets of 964 and 400 images, respectively.

The image data sets obtained by satellite are usually coupled with and supported by other data such as temperature, rainfall and weather data. For example, Cogato et al. [45] picked two Sentinel-2 images best suited for their study. In the study of Kotikot et al. [136], their observations spread over 41 MODIS pixels. Each pixel value from MODIS or Landsat data describes a specific portion of the landscape [45,136]. Therefore, it is quite common to use a relatively small data set. In other studies, the data sets have been constructed by taking a time-series of the images to observe the changes [90,100].

As shown in Table 3 only about half of the studies explicitly mentioned the details about the data sets. Overall, the data sets used are diverse, relatively small, crop specific, various modalities, and designed for specific applications. Consequently, a direct combination of multiple data sets to form a large data set may not be suitable for computational learning methods.

11. Discussion

To predict the expected yield from frost events, real-time information of crops is a crucial step. Visual assessment is time-consuming and labour-intensive, yet potentially subjective. Automation in agriculture allows remote sensing to evaluate frost stress in plants and crops. Moreover, imaging is a non-contact and non-invasive approach to assess frost in real-time. In this sense, hyperspectral and thermal imaging has been demonstrated for the early detection of frost in plants. This is indeed critical, as frost can result in severe head and stem damage in wheat, reducing the quality of the grains and yields by up to 80% [10]. As indicated by the Grains Research and Development Corporation (GRDC) Australia, currently, there are no tools available to map the extent of frost damage other than visual assessment [10]. Farmers usually assess their crops visually soon after a frost event. However, current farm practice in a severe frost event is to cut the crops to produce fodder, or with frost events at the very early stages of plant growth, resow with another crop. Therefore, real-time information on the spatial extent of frost damage in paddocks would greatly benefit farmers. This knowledge will enable them to make decisions for selective harvesting and better management, i.e. manipulating flowering dates, identifying frost-prone paddocks, and selecting appropriate crops for more frost-adverse areas. Both hyperspectral and thermal imaging could provide a routine tool for detecting frost early. Besides facilitating the farmer's crop management decisions, this would also minimize the economic loss of the agriculture industry. These image modalities can be adopted in high-throughput facilities to ensure accurate frost-stress monitoring.

It should also be noted that different image modality is helpful from different research perspectives in detecting frost. For example, thermal imaging can screen the temperature inside the plants, which makes it an essential research element from a physiological and climate science perspective. However, it is unlikely to be of value for industry (when thermal imaging is applied exclusively), as freezing in plants does not necessarily indicate damage. To bridge this gap, thermal imaging combined with other image modalities such as hyperspectral and chlorophyll fluorescence may respond better to pick up the frost-related damage. It is also extremely important to consider the industry requirements for post-event frost-damage identification. In the agricultural industry, an understanding of the temperature dynamics in the paddocks is a real need. Moreover, a drone-based or ground-based multi-modal imaging system may pick up valuable information to map post-frost damage in crops. These gaps open new research opportunities.

However, further research is necessary to address the challenges of employing thermal and hyperspectral imaging in wide-scale agriculture [137]. These facilities may include high-resolution sensors and automated or robot-assisted equipment to capture large-scale images. There is considerable scope for innovative technologies for fine resolutions and automated platforms. Most of the papers covered manual image acquisition and low to mid resolution cameras in the reviewed articles. Additional challenges such as variations in illumination and background as well as mounting platforms need to be adequately addressed. In these contexts, there are still opportunities for future research.

In crop-stress monitoring, deep learning is still a novel approach. Visible physiological changes in crops also occur due to biotic and abiotic stresses other than frost [138]. It is difficult to detect frost damage early when symptoms are not visible to the human eye. According to the Food and Agriculture Organization (FAO), early frost protection and management is the key to reduce frost damage in crops [139]. Deep learning-based imaging techniques can overcome this limitation. For both laboratory and field-scale testing, deep learning can detect and quantify frost damage in plants. Therefore, machine learning has a high potential to detect frost early, but currently, they are not fully utilised. Moreover, there is a significant gap in research for applying deep learning and imaging for frost detection in plants. We observed that DL had outperformed the traditional ML techniques in both speed and accuracy from the papers we reviewed. According to our literature review, it is evident that the accuracy of ML is not yet sufficient in terms of detecting frost damage. To the best of our understanding, there is still an excellent opportunity to refine the ML algorithms to have better performance and accuracy. Besides that, ML and DL technology is still developing; therefore, there is scope for improvement in technical aspects.

Please cite this article as: S. Shammi, F. Sohel, D. Diepeveen et al., A survey of image-based computational learning techniques for frost detection in plants, Information Processing in Agriculture, https://doi.org/10.1016/j.inpa.2022.02.003

One major challenge for improving machine learning applications or deep learning is the lack of publicly available labelled data sets. To the best of our knowledge, there are no public data sets available for detecting frost damage in crops. While there exist some public data sets for agricultural research, e.g. Plant Village [140], EdenPA, Eden library, they focus on diseases, weeds, pests and nutritional deficiencies in various crops. To further advance ML/DL-based frost detection research, the availability of appropriately labelled large image data sets is a necessary requirement. Another challenge is that manually labelling the images is time-consuming and costly. To overcome this, crowd- sourcing could be an option to label an image data set. From our literature review, we noticed that no publication in this area used a large labelled public data set for their work. In every case, the researchers used small data sets they had manually labelled. In that sense, their research could have been expanded a lot more only if there was a large, labelled data set. Therefore, further research is required to put more effort into automatic labelling techniques. The biggest challenge here is achieving the same performance level as humans in this task. Nevertheless, the automatic annotation would reduce the time for manual labelling. In this case, machine learning could provide automatically annotated data that would make the task easier.

A comprehensive performance evaluation of these techniques would have been important in establishing a competitive benchmark. However, the lack of available public data sets is a key challenge in this regard. A future study could construct a comprehensive benchmark data set that contains data from multimodal sensors, multiple crops, and multiple geo-locations. This data set could then be used in new research as well as benchmarking existing techniques.

With the evolution of high-performance CPUs and GPUs, artificial intelligence is contributing to agricultural technologies. Such innovative approaches of deep learning assisted imaging will bring automation to frost-damage detection techniques. However, real-time sensing and monitoring facilities need to be implemented on low-power, low-performance embedded systems for the broader deployment of such technology. For a larger-scale agricultural production, automation for detecting and mapping frost-damaged areas is a necessity. This would allow remotely sensed large scale data to be processed for automatic decision support. This context gives rise to research scopes for efficient communication protocols and cyber-security. However, handling and securely storing large scale data sets is also a challenge. According to a report from FAO, information and automated decision of the early signs and sector- specific risks in agriculture would build resilience in risk management, and food security [141]. However, there are still challenges, such as image acquisition in natural conditions in the field. Moreover, optimisation of the parameters used in deep learning training models is also a challenge.

12. Conclusion

In this survey, we studied imaging-based approaches for frost damage detection analysis in plants. We reviewed 80 relevant papers based on their methodology and data modality. We identified three computational learning approaches, namely statistical, traditional machine learning and deep learning, used for image-based analysis in the reviewed papers. This article proposes a novel taxonomy based on the research studies, which enabled the effective categorisation of all the relevant papers. We also discussed different image modalities that can provide insight into frost in plants. We found that data acquisition technologies have evolved from typical RGB to hyperspectral via infrared and thermal imagery over the last decade. In addition, there have been changes in the deployment of data acquisition sensors from handheld, to fixed mounted, to moving platforms and flying drone imagery. Overall, we have observed a growth in image-based frost detection analysis publications, where computational approaches such as ML and DL are now leading. We anticipate that the availability of large public data sets for a variety of crops and wild plants would trigger further high-quality research in this field. However, some research questions still need to be addressed. Such as, will readily available ML software encourage the agricultural industry and farmers to take up this technology? Will a tailored, robust and targeted, low resource ML software can screen frost before any visual symptoms? In this context, multiple modalities such as thermal, spectral, and RGB can provide complementary and significant data corrections that can be very useful in high performing frost detection. Such multi-modal ML/DL techniques could be the way to improve the results further. Therefore, to improve real-time agricultural frost detection applications, future studies incorporating multi-modal imaging-assisted deep learning algorithms should be conducted for determining the critical temperatures for freezing in plants.

Declaration of Competing Interest

The authors declare that they have no known competing financial interests or personal relationships that could have appeared to influence the work reported in this paper.

Acknowledgement

This work was supported by a Murdoch University Digital Agriculture Connectivity PhD scholarship to Sayma Shammi.

REFERENCES

[1] Hunter MC, Smith RG, Schipanski ME, Atwood LW, Mortensen DA. Agriculture in 2050: recalibrating targets for sustainable intensification. Bioscience 2017;67:386–91.
[2] Jha K, Doshi A, Patel P, Shah M. A comprehensive review on automation in agriculture using artificial intelligence. Artif Intell Agric 2019;2:1–12.
[3] Imam SA, Choudhary A, Sachan VK. Design issues for wireless sensor networks and smart humidity sensors for precision agriculture: a review. In: 2015 int conf soft comput tech implementations; 2015. p. 181–7.
[4] Augspurger CK. Reconstructing patterns of temperature, phenology, and frost damage over 124 years: spring damage risk is increasing. Ecology 2013;94(1):41–50.

[5] Bjerke JW, Tømmervik H, Zielke M, Jørgensen M. Impacts of snow season on ground-ice accumulation, soil frost and primary productivity in a grassland of sub-Arctic Norway. Environ Res Lett 2015;10(9):095007. https://doi.org/10.1088/1748-9326/10/9/095007.
[6] Jones HG. Frost protection: fundamentals, practice, and economics. Volume 1. By RL Snyder and JP de Melo-Abreu. Rome: FAO (2005), pp. 223, US $38.00. ISBN 92-5-105328-6; Volume 2. By RL Snyder, JP de Melo-Abreu and S. Matulich. Rome: FAO (2005), pp. 64. US $24.00. Exp Agric 2006;42:369.
[7] Papagiannaki K, Lagouvardos K, Kotroni V, Papagiannakis G. Agricultural losses related to frost events: Use of the 850 hPa level temperature as an explanatory variable of the damage cost. Nat Hazards Earth Syst Sci 2014;14:2375–86.
[8] Faust E, Herbold J. Spring frost losses and climate change–not a contradiction in terms. Munich RE. <https//Www Munichre Com/Topics-Online/En/Climate-Change-and-Natural-Disasters/Climate-Change/Spring-Frost-Losses-Climate-Change-2018html> [accessed 2018;16].
[9] March T, Knights S, Biddulph B, Ogbonnaya F, Maccallum R, Belford RK. The GRDC national frost initiative. GRDC Updat Pap 2015.
[10] Fitzgerald GJ, Perry EM, Jones H, Stutsel BM, Nuttall JG, Wallace A, et al. Quantification of frost damage in grains using remote sensing; 2020.
[11] Stutsel BM, Callow JN, Flower KC, Biddulph T Ben, Issa NA. Application of distributed temperature sensing using optical fibre to understand temperature dynamics in wheat (triticum aestivum) during frost. Eur J Agron 2020;115:126038.
[12] Nuttall JG, Perry EM, Delahunty AJ, O'Leary GJ, Barlow KM, Wallace AJ. Frost response in wheat and early detection using proximal sensors. J Agron Crop Sci 2019;205:220–34.
[13] Perry E, Nuttall J, Wallace A, Delahunty A, Barlow K, others. Evaluating canopy reflectance for assessment of frost damage in wheat. In: Doing more with less, Proc 18th Aust Agron Conf 2017, Ballarat, Victoria, Aust 24–28 Sept. 2017; 2017. p. 1–4.
[14] Wisniewski M, Lindow SE, Ashworth EN. Observations of ice nucleation and propagation in plants using infrared video thermography. Plant Physiol 1997;113:327–34.
[15] Workmaster BAA, Palta JP, Wisniewski M. Ice nucleation and propagation in cranberry uprights and fruit using infrared video thermography. J Am Soc Hortic Sci 1999;124:619–25.
[16] Mishra A, Heyer AG, Mishra KB. Chlorophyll fluorescence emission can screen cold tolerance of cold acclimated Arabidopsis thaliana accessions. Plant Methods 2014;10:1–10.
[17] Asante EA, Du Z, Lu Y, Hu Y. Detection and assessment of nitrogen effect on cold tolerance for tea by hyperspectral reflectance with PLSR, PCR, and LM models. Inf Process Agric 2021;8:96–104.
[18] Fernandez-Gallego JA, Kefauver SC, Vatter T, Gutiérrez NA, Nieto-Taladriz MT, Araus JL. Low-cost assessment of grain yield in durum wheat using RGB images. Eur J Agron 2019;105:146–56.
[19] Fitzgerald GJ, Perry EM, Flower KC, Nikolaus Callow J, Boruff B, Delahunty A, et al. Frost damage assessment in wheat using spectral mixture analysis. Remote Sens 2019;11.
[20] Murphy ME, Boruff B, Callow JN, Flower KC. Detecting frost stress in wheat: A controlled environment hyperspectral study on wheat plant components and implications for multispectral field sensing. Remote Sens 2020;12:477.
[21] Fennell A. Freezing tolerance and injury in grapevines. J Crop Improv 2004;10:201–35.
[22] Neuner G. Frost resistance in alpine woody plants. Front Plant Sci 2014;5:654.
[23] Ambroise V, Legay S, Guerriero G, Hausman J-F, Cuypers A, Sergeant K. The roots of plant frost hardiness and tolerance. Plant Cell Physiol 2020;61:3–20.
[24] Humplík JF, Lazár D, Husičková A, Spíchal L. Automated phenotyping of plant shoots using imaging methods for analysis of plant stress responses–a review. Plant Methods 2015;11:1–10.
[25] Yu DJ, Lee HJ. Evaluation of freezing injury in temperate fruit trees. Hortic Environ Biotechnol 2020:1–8.
[26] Gao Z, Luo Z, Zhang W, Lv Z, Xu Y. Deep learning application in plant stress imaging: a review. Agri Eng 2020;2:430–46.
[27] Barlow KM, Christy BP, O'leary GJ, Riffkin PA, Nuttall JG. Simulating the impact of extreme heat and frost events on wheat crop production: a review. F Crop Res 2015;171:109–19.
[28] Kolhar S, Jagtap J. Plant trait estimation and classification studies in plant phenotyping using machine vision-a review. Inf Process Agric 2021.
[29] Pineda M, Barón M, Pérez-Bueno M-L. Thermal imaging for plant stress detection and phenotyping. Remote Sens 2021;13:68.
[30] Stier JC, Filiault DL, Wisniewski M, Palta JP. Visualization of freezing progression in turfgrasses using infrared video thermography. Crop Sci 2003;43:415–20.
[31] Pearce RS, Fuller MP. Freezing of barley studied by infrared video thermography. Plant Physiol 2001;125:227–40.
[32] Ceccardi TL, Heath RL, Ting IP. Low-temperature exotherm measurement using infrared thermography. HortScience 1995;30:140–2.
[33] Wisniewski M, Glenn DM, Fuller MP. Use of a hydrophobic particle film as a barrier to extrinsic ice nucleation in tomato plants. J Am Soc Hortic Sci 2002;127:358–64.
[34] Andonova A, Andreev A. Software for computerized thermal image processing. Proc 10th EC 2009:108–11.
[35] Livingston III DP, Tuong TD, Isleib TG, Murphy JP. Differences between wheat genotypes in damage from freezing temperatures during reproductive growth. Eur J Agron 2016;74:164–72.
[36] Al-Issawi M, Rihan HZ, El-Sarkassy N, Fuller MP. Frost hardiness expression and characterisation in wheat at ear emergence. J Agron Crop Sci 2013;199:66–74.
[37] Hacker J, Ladinig U, Wagner J, Neuner G. Inflorescences of alpine cushion plants freeze autonomously and may survive subzero temperatures by supercooling. Plant Sci 2011;180:149–56.
[38] Stegner M, Schäfernolte T, Neuner G. New insights in potato leaf freezing by Infrared Thermography. Appl Sci 2019;9:819.
[39] Kishimoto T, Yamazaki H, Saruwatari A, Murakawa H, Sekozawa Y, Kuchitsu K, et al. High ice nucleation activity located in blueberry stem bark is linked to primary freeze initiation and adaptive freezing behaviour of the bark. AoB Plants 2014;6.
[40] Livingston DP, Tuong TD, Murphy JP, Gusta LV, Willick I, Wisniewski ME. High-definition infrared thermography of ice nucleation and propagation in wheat under natural frost conditions and controlled freezing. Planta 2018;247:791–806.
[41] Neuner G, Kreische B, Kaplenig D, Monitzer K, Miller R. Deep supercooling enabled by surface impregnation with lipophilic substances explains the survival of overwintering buds at extreme freezing. Plant Cell Environ 2019;42:2065–74.
[42] Hoermiller II, Ruschhaupt M, Heyer AG. Mechanisms of frost resistance in Arabidopsis thaliana. Planta 2018;248:827–35.
[43] Kokin E, Pennar M, Palge V, Jürjenson K. Strawberry leaf surface temperature dynamics measured by thermal camera in night frost conditions; 2018.

Please cite this article as: S. Shammi, F. Sohel, D. Diepeveen et al., A survey of image-based computational learning techniques for frost detection in plants, Information Processing in Agriculture, https://doi.org/10.1016/j.inpa.2022.02.003

[44] Yuan W, Choi D. UAV-based heating requirement determination for frost management in apple orchard. Remote Sens 2021;13:273.
[45] Cogato A, Meggio F, Collins C, Marinello F. Medium-resolution multispectral data from sentinel-2 to assess the damage and the recovery time of late frost on vineyards. Remote Sens 2020;12:1896.
[46] Jełowicki Ł, Sosnowicz K, Ostrowski W, Osińska-Skotak K, Bakuła K. Evaluation of rapeseed winter crop damage using UAV-based multispectral imagery. Remote Sens 2020;12:2618.
[47] Goswami J, Sharma V, Chaudhury BU, Raju PLN. Rapid identification of abiotic stress (frost) in in-filed maize crop using UAV remote sensing. Int Arch Photogramm Remote Sens & Spat Inf Sci 2019.
[48] Lacoste C, Nansen C, Thompson S, Moir-Barnetson L, Mian A, McNee M, et al. Increased susceptibility to aphids of flowering wheat plants exposed to low temperatures. Environ Entomol 2015;44:610–8.
[49] Wei C, Huang J, Wang X, Blackburn GA, Zhang Y, Wang S, et al. Hyperspectral characterization of freezing injury and its biochemical impacts in oilseed rape leaves. Remote Sens Environ 2017;195:56–66.
[50] Feng M, Guo X, Wang C, Yang W, Shi C, Ding G, et al. Monitoring and evaluation in freeze stress of winter wheat (Triticum aestivum L.) through canopy hyperspectrum reflectance and multiple statistical analysis. Ecol Indic 2018;84:290–7.
[51] Lu Y, Walker TD, Acosta JJ, Young S, Pandey P, Heine AJ, et al. Prediction of freeze damage and minimum winter temperature of the seed source of loblolly pine seedlings using hyperspectral imaging. For Sci 2021.
[52] Zhang J, Dai L, Cheng F. Classification of frozen corn seeds using hyperspectral VIS/NIR reflectance imaging. Molecules 2019;24:149.
[53] Yang W, Yang C, Hao Z, Xie C, Li M. Diagnosis of plant cold damage based on hyperspectral imaging and convolutional neural network. IEEE Access 2019;7:118239–48.
[54] Shao Y, Gao C, Xuan G, Gao X, Chen Y, Hu Z. Determination of damaged wheat kernels with hyperspectral imaging analysis. Int J Agric Biol Eng 2020;13:194–8.
[55] Gao Z, Zhao Y, Khot LR, Hoheisel G-A, Zhang Q. Optical sensing for early spring freeze related blueberry bud damage detection: Hyperspectral imaging for salient spectral wavelengths identification. Comput Electron Agric 2019;167:105025.
[56] Choudhury BU, Webster R, Sharma V, Goswami J, Meetei TT, Krishnappa R, et al. Frost damage to maize in northeast India: assessment and estimated loss of yield by hyperspectral proximal remote sensing. J Appl Remote Sens 2019;13:44527.
[57] Lee WSL, Ferrante A, Withayachumnankul W, Able JA. Assessing frost damage in barley using terahertz imaging. Opt Exp 2020;28:30644–55.
[58] Agelet LE, Ellis DD, Duvick S, Goggi AS, Hurburgh CR, Gardner CA. Feasibility of near infrared spectroscopy for analyzing corn kernel damage and viability of soybean and corn kernels. J Cereal Sci 2012;55:160–5.
[59] Jia S, Yang L, An D, Liu Z, Yan Y, Li S, et al. Feasibility of analyzing frost-damaged and non-viable maize kernels based on near infrared spectroscopy and chemometrics. J Cereal Sci 2016;69:145–50.
[60] Wu Y, Ma Y, Hu X, Ma J, Zhao H, Ren D. Narrow-waveband spectral indices for prediction of yield loss in frost-damaged winter wheat during stem elongation. Eur J Agron 2021;124:126240.
[61] Macedo-Cruz A, Pajares G, Santos M, Villegas-Romero I. Digital image sensor-based assessment of the status of oat (Avena sativa L.) crops after frost damage. Sensors 2011;11:6015–36.
[62] HamidiSepehr A, Mirnezami SV, Ward JK. Comparison of object detection methods for corn damage assessment using deep learning. Trans ASABE 2020;63:1969–80.
[63] López-Granados F, Torres-Sánchez J, Jiménez-Brenes FM, Arquero O, Lovera M, De Castro AI. An efficient RGB-UAV-based platform for field almond tree phenotyping: 3-D architecture and flowering traits. Plant Methods 2019;15:1–16.
[64] Kimball JA, Tuong TD, Arellano C, Livingston III DP, Milla-Lewis SR. Assessing freeze-tolerance in St. Augustinegrass: temperature response and evaluation methods. Euphytica 2017;213:110.
[65] Perry EM, Nuttall JG, Wallace AJ, Fitzgerald GJ. In-field methods for rapid detection of frost damage in Australian dryland wheat during the reproductive and grain-filling phase. Crop Pasture Sci 2017;68:516–26.
[66] Livingston III DP, Henson CA, Tuong TD, Wise ML, Tallury SP, Duke SH. Histological analysis and 3D reconstruction of winter cereal crowns recovering from freezing: a unique response in oat (Avena sativa L.). PLoS One 2013;8:e53468.
[67] Dong Z, Men Y, Liu Z, Li J, Ji J. Application of chlorophyll fluorescence imaging technique in analysis and detection of chilling injury of tomato seedlings. Comput Electron Agric 2020;168:105109.
[68] Arnold PA, Briceño VF, Gowland KM, Catling AA, Bravo LA, Nicotra AB. A high-throughput method for measuring critical thermal limits of leaves by chlorophyll imaging fluorescence. BioRxiv 2020.
[69] Gorbe E, Calatayud A. Applications of chlorophyll fluorescence imaging technique in horticultural research: a review. Sci Hortic (Amsterdam) 2012;138:24–35.
[70] Dong Z, Men Y, Li Z, Zou Q, Ji J. Chlorophyll fluorescence imaging as a tool for analyzing the effects of chilling injury on tomato seedlings. Sci Hortic (Amsterdam) 2019;246:490–7.
[71] Mishra A, Mishra KB, Höermiller II, Heyer AG, Nedbal L. Chlorophyll fluorescence emission as a reporter on cold tolerance in Arabidopsis thaliana accessions. Plant Signal Behav 2011;6:301–10.
[72] Qian J, Zhou J, Gong R, Liu Y, Zhang G. Freezing resistance evaluation of rose stems during frost dehardening using electrical impedance tomography. BMC Plant Biol 2021;21:1–12.
[73] Stegner M, Wagner J, Neuner G. Ice accommodation in plant tissues pinpointed by cryo-microscopy in reflected-polarised-light. Plant Methods 2020;16:1–9.
[74] Borompichaichartkul C, Moran G, Srzednicki G, Price WS. Nuclear magnetic resonance (NMR) and magnetic resonance imaging (MRI) studies of corn at subzero temperatures. J Food Eng 2005;69:199–205.
[75] Liu W, Zhang X, He F, Xiong Q, Zan X, Liu Z, et al. Open-air grape classification and its application in parcel-level risk assessment of late frost in the eastern Helan Mountains. ISPRS J Photogramm Remote Sens 2021;174:132–50.
[76] Cheng F, Zhang J, Dai L. Method for identifying frostbite condition of grain seeds using spectral feature wavebands of seed embryo hyperspectral images; 2020.
[77] Adisa OM, Botai JO, Adeola AM, Hassen A, Botai CM, Darkey D, et al. Application of artificial neural network for predicting maize production in South Africa. Sustainability 2019;11:1145.
[78] She B, Huang J, Guo R, Wang H, Wang J. Assessing winter oilseed rape freeze injury based on Chinese HJ remote sensing data. J Zhejiang Univ B 2015;16:131–44.
[79] Xie Y, Wang C, Yang W, Feng M, Qiao X, Song J. Canopy hyperspectral characteristics and yield estimation of winter

Please cite this article as: S. Shammi, F. Sohel, D. Diepeveen et al., A survey of image-based computational learning techniques for frost detection in plants, Information Processing in Agriculture, https://doi.org/10.1016/j.inpa.2022.02.003

wheat (Triticum aestivum) under low temperature injury. Sci Rep 2020;10:1–10.
[80] Enders TA, St. Dennis S, Oakland J, Callen ST, Gehan MA, Miller ND, et al. Classifying cold-stress responses of inbred maize seedlings using RGB imaging. Plant Direct 2019;3: e00104.
[81] Ma J, Li Y, Du K, Zheng F, Zhang L, Gong Z, et al. Segmenting ears of winter wheat at flowering stage using digital images and deep learning. Comput Electron Agric 2020;168:105159.
[82] Cho N, Kang S, Lee B, Agossou C, Lee J, Lim J-H, et al. Mapping satellite-derived thermal parameters of canopy onset and assessing their temperature dependency for temperate forests in Korea. Ecol Indic 2021;125:107528.
[83] Zhang L, Sun H, Rao Z, Ji H. Hyperspectral imaging technology combined with deep forest model to identify frost-damaged rice seeds. Spectrochim Acta Part A Mol Biomol Spectrosc 2020;229:117973.
[84] Duddu HSN, Pajic V, Noble SD, Tanino KK, Shirtliffe SJ. Image-based rapid estimation of frost damage in canola (Brassica napus l.). Can J Remote Sens 2018;44:169–75.
[85] Singh A, Ganapathysubramanian B, Singh AK, Sarkar S. Machine learning for high-throughput stress phenotyping in plants. Trends Plant Sci 2016;21:110–24.
[86] Hira ZM, Gillies DF. A review of feature selection and feature extraction methods applied on microarray data. Adv Bioinformatics 2015; 2015.
[87] Bodapati JD, Veeranjaneyulu N. Feature extraction and classification using deep convolutional neural networks. J Cyber Secur Mobil 2018:261–76.
[88] Liang J, others. Spectral-spatial Feature Extraction for Hyperspectral Image Classification; 2016.
[89] Wang S, Chen J, Rao Y, Liu L, Wang W, Dong Q. Response of winter wheat to spring frost from a remote sensing perspective: Damage estimation and influential factors. ISPRS J Photogramm Remote Sens 2020;168:221–35.
[90] Kotikot SM, Flores A, Griffin RE, Nyaga J, Case JL, Mugo R, et al. Statistical characterization of frost zones: Case of tea freeze damage in the Kenyan highlands. Int J Appl Earth Obs Geoinf 2020;84:101971.
[91] Bascietto M, Bajocco S, Mazzenga F, Matteucci G. Assessing spring frost effects on beech forests in Central Apennines from remotely-sensed data. Agric For Meteorol 2018;248:240–50.
[92] Sharma A, Sharma A. Machine learning: a review of techniques of machine learning. JASC J Appl Sci Comput 2018;5:538–41.
[93] Patterson J, Gibson A. Deep learning: A practitioner's approach. O'Reilly Media, Inc.; 2017.
[94] Minet J, Curnel Y, Gobin A, Goffart J-P, Melard F, Tychon B, et al. Crowdsourcing for agricultural applications: A review of uses and opportunities for a farmsourcing approach. Comput Electron Agric 2017;142:126–38.
[95] Van Etten J, Beza E, Calderer L, Van Duijvendijk K, Fadda C, Fantahun B, et al. First experiences with a novel farmer citizen science approach: Crowdsourcing participatory variety selection through on-farm triadic comparisons of technologies (tricot). Exp Agric 2019;55:275–96.
[96] Høye G, Løke T, Fridman A. Method for quantifying image quality in push-broom hyperspectral cameras. Opt Eng 2015;54:53102.
[97] Zhang J, Dai L, Cheng F. Identification of corn seeds with different freezing damage degree based on hyperspectral reflectance imaging and deep learning method. Food Anal Methods 2021;14:389–400.
[98] Wong CP, Subramaniam R. Use of technology in biology education–case of infrared thermal imaging. J Biol Educ 2020:1–13.
[99] Kotikot SM, Onywere SM. Application of GIS and remote sensing techniques in frost risk mapping for mitigating agricultural losses in the Aberdare ecosystem. Kenya. Geocarto Int 2015;30:104–21.
[100] Currit N, St Clair SB. Assessing the impact of extreme climatic events on aspen defoliation using MODIS imagery. Geocarto Int 2010;25:133–47.
[101] Fayad I, Baghdadi N, Bazzi H, Zribi M. Near real-time freeze detection over agricultural plots using Sentinel-1 data. Remote Sens 2020;12:1976.
[102] Gobbett DL, Nidumolu U, Crimp S. Modelling frost generates insights for managing risk of minimum temperature extremes. Weather Clim Extrem 2020;27:100176.
[103] Sun Z, Wang X, Yamamoto H, Zhang J, Tani H, Zhong G, et al. Extraction of rice-planting area and identification of chilling damage by remote sensing technology: a case study of the emerging rice production region in high latitude. Paddy Water Environ 2017;15:181–91.
[104] Zhao L, Li Q, Zhang Y, Wang H, Du X. Normalized NDVI valley area index (NNVAI)-based framework for quantitative and timely monitoring of winter wheat frost damage on the Huang-Huai-Hai Plain, China. Agric Ecosyst Environ 2020;292:106793.
[105] Becker-Reshef I, Vermote E, Lindeman M, Justice C. A generalized regression-based model for forecasting winter wheat yields in Kansas and Ukraine using MODIS data. Remote Sens Environ 2010;114:1312–23.
[106] Chen Y, Sidhu HS, Kaviani M, McElroy MS, Pozniak CJ, Navabi A. Application of image-based phenotyping tools to identify QTL for in-field winter survival of winter wheat (Triticum aestivum L.). Theor Appl Genet 2019;132:2591–604.
[107] Ackar H, Abd Almisreb A, Saleh MA. A review on image enhancement techniques. Southeast Eur J Soft Comput 2019;8.
[108] Liu Z, Liu H, Luo C, Yang H, Meng X, Ju Y, et al. Rapid extraction of regional-scale agricultural disasters by the standardized monitoring model based on google earth engine. Sustainability 2020;12:6497.
[109] Gwet DLL, Otesteanu M, Libouga IO, Bitjoka L, Popa GD. A review on image segmentation techniques and performance measures. Int J Comput Inf Eng 2018;12:1107–17.
[110] Hichri H, Bazi Y, Alajlan N, Malek S. Interactive segmentation for change detection in multispectral remote-sensing images. IEEE Geosci Remote Sens Lett 2012;10:298–302.
[111] Chen J, Shao H, Hu C. Image segmentation based on mathematical morphological operator. Color Image Process 2017.
[112] Mutlag WK, Ali SK, Aydam ZM, Taher BH. Feature extraction methods: a review. J Phys Conf Ser 2020;1591:12028.
[113] Zebari R, Abdulazeez A, Zeebaree D, Zebari D, Saeed J. A Comprehensive review of dimensionality reduction techniques for feature selection and feature extraction. J Appl Sci Technol Trends 2020;1:56–70.
[114] Ye X, Sakai K, Okamoto H, Garciano LO. A ground-based hyperspectral imaging system for characterizing vegetation spectral features. Comput Electron Agric 2008;63:13–21.
[115] Abdel-Rahman EM, Mutanga O, Odindi J, Adam E, Odindo A, Ismail R. A comparison of partial least squares (PLS) and sparse PLS regressions for predicting yield of Swiss chard grown under different irrigation water sources using hyperspectral data. Comput Electron Agric 2014;106:11–9.
[116] Upadhyay R, Panse P, Soni A, Rathore BU. Principal component analysis as a dimensionality reduction and data preprocessing technique. Proc Recent Adv Interdiscip Trends Eng Appl 2019.

Please cite this article as: S. Shammi, F. Sohel, D. Diepeveen et al., A survey of image-based computational learning techniques for frost detection in plants, Information Processing in Agriculture, https://doi.org/10.1016/j.inpa.2022.02.003

[117] Vyse K, Penzlin J, Sergeant K, Hincha DK, Arora R, Zuther E. Repair of sub-lethal freezing damage in leaves of Arabidopsis thaliana. BMC Plant Biol 2020;20:1–18.
[118] Chu B, Yu K, Zhao Y, He Y. Development of noninvasive classification methods for different roasting degrees of coffee beans using hyperspectral imaging. Sensors 2018;18:1259.
[119] Yang W, Wang K, Zuo W. Neighborhood component feature selection for high-dimensional data. JCP 2012;7:161–8.
[120] Leutenegger S, Chli M, Siegwart RY. BRISK: binary robust invariant scalable keypoints. 2011 Int Conf Comput Vis 2011:2548–55.
[121] Jogin M, Madhulika MS, Divya GD, Meghana RK, Apoorva S, others. Feature extraction using convolution neural networks (CNN) and deep learning. In: 2018 3rd IEEE Int Conf Recent Trends Electron Inf Commun Technol; 2018. p. 2319–23.
[122] St L, Wold S, et al. Analysis of variance (ANOVA). Chemom Intell Lab Syst 1989;6:259–72.
[123] Vetter TR. Descriptive statistics: reporting the answers to the 5 basic questions of who, what, why, when, where, and a sixth, so what? Anesth Analg 2017;125:1797–802.
[124] Takeda F, Glenn DM, et al. Susceptibility of blackberry flowers to freezing temperatures. Eur J Hortic Sci 2016;81:15–121.
[125] Lai Y. A comparison of traditional machine learning and deep learning in image recognition. J Phys Conf Ser 2019;1314:12148.
[126] Colas F, Brazdil P. On the behavior of svm and some older algorithms in binary text classification tasks. Int. Conf. Text, Speech Dialogue; 2006. p. 45–52.
[127] Cortes C, Vapnik V. Support-vector networks. Mach Learn 1995;20:273–97.
[128] Cervantes J, Garcia-Lamont F, Rodríguez-Mazahua L, Lopez A. A comprehensive survey on support vector machine classification: applications, challenges and trends. Neurocomputing 2020;408:189–215.
[129] Bao S, Jingfeng H, Dongyan Z, Linsheng H. Assessing and characterizing oilseed rape freezing injury based on MODIS and MERIS data. Int J Agric Biol Eng 2017;10:143–57.
[130] Breiman L. Random forests. Mach Learn 2001;45:5–32.
[131] Bochkovskiy A, Wang C-Y, Liao H-YM. Yolov4: Optimal speed and accuracy of object detection. ArXiv Prepr ArXiv200410934; 2020.
[132] Smucker MD, Allan J, Carterette B. A comparison of statistical significance tests for information retrieval evaluation. Proc Sixt ACM Conf Conf Inf Knowl Manag 2007:623–32.
[133] Hossin M, Sulaiman MN. A review on evaluation metrics for data classification evaluations. Int J Data Min Knowl Manag Process 2015;5:1.
[134] Staôpor K. Evaluating and comparing classifiers: Review, some recommendations and limitations. Int Conf Comput Recognit Syst 2017:12–21.
[135] Lu Y, Payn KG, Pandey P, Acosta JJ, Heine AJ, Walker TD, et al. ASABE Annu. Int. Virtual Meet. 2020;2020:1.
[136] Kotikot SM, Flores A, Griffin RE, Sedah A, Nyaga J, Mugo R, et al. Mapping threats to agriculture in East Africa: Performance of MODIS derived LST for frost identification in Kenya's tea plantations. Int J Appl Earth Obs Geoinf 2018;72:131–9.
[137] Khanal S, Fulton J, Shearer S. An overview of current and potential applications of thermal remote sensing in precision agriculture. Comput Electron Agric 2017;139:22–32.
[138] Anami BS, Malvade NN, Palaiah S. Classification of yield affecting biotic and abiotic paddy crop stresses using field images. Inf Process Agric 2020;7:272–85.
[139] Snyder RL, Melo Abreu JP de, others. Frost protection: fundamentals, practice and economics. FAO, Roma (Italia); 2005.
[140] Lu Y, Young S. A survey of public datasets for computer vision tasks in precision agriculture. Comput Electron Agric 2020;178:105760.
[141] Gitz V, Meybeck A, Lipper L, De YC, Braatz S. Climate change and food security: risks and responses. Food Agric Organ United Nations Rep 2016;110.
[142] Peng O, Akers W, Berezin MY. Detection of Cold Stress in Plants using Fluorescence Lifetime Imaging (FLIM). Curr Anal Chem 2021;17:317–27.
[143] Bao Y, Mi C, Wu N, Liu F, He Y. Rapid Classification of wheat grain varieties using hyperspectral imaging and chemometrics. Appl Sci 2019;9:4119.
[144] Liu J, Lindstrom OM, Chavez DJ. Differential thermal analysis of 'Elberta'and 'Flavorich'Peach flower buds to predict cold hardiness in Georgia. HortScience 2019;54:676–83.
[145] Nolè A, Rita A, Ferrara AMS, Borghetti M. Effects of a large-scale late spring frost on a beech (Fagus sylvatica L.) dominated Mediterranean mountain forest derived from the spatio-temporal variations of NDVI. Ann For Sci 2018;75:1–11.
[146] Prabhakara K, Hively WD, McCarty GW. Evaluating the relationship between biomass, percent groundcover and remote sensing indices across six winter cover crop fields in Maryland, United States. Int J Appl Earth Obs Geoinf 2015;39:88–102.
[147] Su L, Dai Z, Li S, Xin H. A novel system for evaluating drought–cold tolerance of grapevines using chlorophyll fluorescence. BMC Plant Biol 2015;15:1–12.
[148] Wu Q, Zhu D, Wang C, Ma Z, Wang J. Diagnosis of freezing stress in wheat seedlings using hyperspectral imaging. Biosyst Eng 2012;112:253–60.
[149] Wang H, Wang J, Wang Q, Miao N, Huang W, Feng H, et al. First Int Conf Agro-Geoinform 2012;2012:1–6.

Please cite this article as: S. Shammi, F. Sohel, D. Diepeveen et al., A survey of image-based computational learning techniques for frost detection in plants, Information Processing in Agriculture, https://doi.org/10.1016/j.inpa.2022.02.003